DESIGN AND CAE ANALYSIS OF REFRIGERATOR DOOR OPENING ASSIST MECHANISM

A Thesis report submitted in partial fulfillment of the requirement for the award of

MASTER OF ENGINEERING

IN

CAD/CAM ENGINEERING

Submitted By

Navtej Singh

Roll No. 801684008

Under the Guidance of

Mr. Sumit Virdi	**Dr. Neeraj Grover**	**Dr. Gagandeep Bhardwaj**
Manager, Refrigerator. Dept.	Assistant Professor,	Assistant Professor,
LG Soft Pvt. Ltd.	Dept. of Mech. Engg	Dept. of Mech. Engg
Greater Noida City,U.P.	TIET,Patiala	TIET,Patiala

DEPARTMENT OF MECHANICAL ENGINEERING

THAPAR INSTITUTE OF ENGINEERING & TECHNOLOGY

PATIALA-147004, INDIA

July-2018

DECLARATION

I hereby declare that work in this thesis report entitled **"DESIGN AND CAE ANALYSIS OF REFRIGERATOR DOOR OPENING ASSIST MECHANISM"** is an authentic record of my study carried out as a requirement for the award of degree of Master of Engineering (CAD/CAM & ROBOTICS) at **THAPAR INSITUTE OF ENGINEERING & TECHNOLOGY, Patiala** under the guidance of **Mr. Sumit Virdi**, Manger, Refrigerator Deptt. at LG Soft Pvt. Ltd., Greater Noida U.P. , **Dr. Neeraj Grover** Assistant Professor Department of Mechanical Engineering, Thapar Institute of Engineering and Technology, Patiala and **Dr. Gagandeep Bhardwaj,** Assistant Professor Department of Mechanical Engineering, Thapar Institute of Engineering and Technology, Patiala. The matter embodied in this report has not been submitted in part or full to any other university or institute for the award of any other degree.

Navtej Singh

Date: 30 July 2018
Place: Patiala.

(Navtej Singh)
Reg. No. 801684008

This is to certify that above declaration made by student concerned is corrected to the best of our knowledge and belief.

LG SOFT INDIA PRIVATE LIMITED GREATER NOIDA

Mr.Sumit Virdi
Manager, Refrigerator. Deptt
LG Soft Pvt. Ltd.
Greater Noida City,U.P.

Dr. Neeraj Grover
Assistant Professor,
Deptt. Of Mech. Engg
TIET,Patiala

Dr. Gagandeep Bhardwaj
Assistant Professor,
Deptt. Of Mech. Engg
TIET,Patiala

DECLARATION

I Hereby declare that work in this thesis report entitled **"DESIGN AND CAE ANALYSIS OF REFRIGERATOR DOOR OPENING ASSIST MECHANISM"** is an authentic record of my study carried out as a requirement for the award of degree of Master of Engineering (CAD/CAM & ROBOTICS) at **THAPAR INSITUTE OF ENGINEERING & TECHNOLOGY, Patiala** under the guidance of **Mr. Sumit Virdi**, Manger, Refrigerator. Deptt at LG Soft Pvt. Ltd., Greater Noida U.P. , **Dr. Neeraj Grover** Assistant Professor Department of Mechanical Engineering, Thapar Institute of Engineering and Technology, Patiala and **Dr. Gagandeep Bhardwaj,** Assistant Professor Department of Mechanical Engineering, Thapar Institute of Engineering and Technology, Patiala. The matter embodied in this report has not been submitted in part or full to any other university or institute for the award of any other degree.

Date: (Navtej Singh)
Place: Reg. No. 801684008

This is to certify that above declaration made by student concerned is corrected to the best of our knowledge and belief.

Mr.Sumit Virdi	**Dr. Neeraj Grover**	**Dr. Gagandeep Bhardwaj**
Manager, Refrigerator. Deptt	**Assistant Professor,**	**Assistant Professor,**
LG Soft Pvt. Ltd.	**Deptt. Of Mech. Engg**	**Deptt. Of Mech. Engg**
Greater Noida City,U.P.	**TIET,Patiala**	**TIET,Patiala**

DEDICATION

To my supportive family, friends, academic teachers and industrial mentor who supported me directly or indirectly through my Post Graduation.

ACKNOWLEDGEMENT

I am highly thankful to my supervisor **Mr. Brijesh Sharma, Deputy General Manager** along with his team for giving me an opportunity to work on this project and moreover, for their indispensable contribution in stimulating suggestions and encouragement. I am highly indebted to them for their invaluable guidance and support not only in my project but also in shaping my attitude towards research and development. Their constant support and encouragement right from the beginning of my journey in LG has been a major motivation and force behind the successful completion of this project.

I express my deep gratitude and thank to my Industrial mentor **Mr. Sumit Virdi**, Manger, Refrigerator. Department at LG Soft Pvt. Ltd. and academic guides **Dr. Neeraj Grover** and **Dr. Gagandeep Bhardwaj**, Assistant Professor Department of Mechanical Engineering, Thapar Institute of Engineering for their invaluable guidance and suggestions, helping me to submit my thesis report in present form.

I would also like to thank **Late Mr. N.K. Jain** (Director Home Appliances India Lab) for permitting me to undergo the internship-training program in Refrigerator Department of LG Home Appliances India lab. Moreover, his keen interest and critical analysis kept me motivated to work and complete the assigned task.

I thank all the employees of LG Soft India, especially **Mr. Vikas Bakshi** for providing me with all the necessary information to make my stay comfortable. I would also like to mention **Mr. Sanjeev Reddy**, as without him and his prototype making team, it would not be possible to complete the project in time.

Last but not the least I would also like to thank all the employees of the company for their kind cooperation in my training.

Sincerely

ABSTRACT

To provide more comfort and ease to customers, there is a need to introduce new ideas for door opening assist mechanism in home appliance industry. In present work, two different mechanisms are designed and analyzed. One a manually operated mechanized handle and other a geared motor actuated automated door push plunger. Initially, the different dimensional parameters were optimized for given a position and size constraint available for the assembly. Multi-body dynamics system approach is used for kinematic and dynamic simulation. The movement of individual part is kinematically and dynamically analyzed for input and output force and displacement of parts. Designed manually mechanized door handle effectively reduces the force required to detach the magnet gasket seal from the steel wall of refrigerator cabinet by certain distance during door opening. Secondly, geared motor actuated automated push plunger is designed in a unique way to obtain the back and forth motion of push plunger without changing the direction of rotation of motor. A worm and worm wheel and three stage gear train spur is designed optimally to fit within the given constraints.

Keywords: Design, Optimization, CAE

CONTENTS

LIST OF FIGURE

LIST OF TABLES

CHAPTER 1 INTRODUCTION

In this chapter the basic details and concepts related to the present work are discussed.

1.1 INTRODUCTION TO PROBLEM

Presently, most of the refrigerators models have conventional fixed door opening handle which is rigidly fixed to the door of refrigerator. The refrigerator door is equipped with a magnet gasket sealing preventing the escape of cold air from inside of refrigerator and freezer cabinet to the outer atmosphere. Magnet gasket sealing consists of NdFeB rubber magnet strip with PVC housing to provide air tight seal. This magnet gasket sealing keeps the door attached to the steel cabinets of the refrigerators. According to Code of Federal Regulations Sub Chapter F-Refrigerator Safety Act Regulations Part 1750, the force applied perpendicularly to the plane of door should not exceed 66.7 Newton (15 pounds) and the required turning moment to turn the door should not be more than 0.57 Newton meter (5 inch-pounds) on the door handle through an angle of rotation of $45^{o}\pm15^{o}$. After the door is detached from the steel cabinet, the free rotation motion is restricted by an ABS snap type stopper assembled with the bottom hinge of the door. The snap type stopper serves two different purposes. Firstly, it restricts the free rotation displacement of the door while opening and secondly, it pushes the door towards the cabinet frame by snap spring action while closing the door.

The user operating the door experiences two type of jerks. One is due to magnetic gasket sealing and other is due to snap type stopper. The magnitude of jerk due to magnetic strip is higher as compared to the jerk due to snap type stopper. The present work provides the solution to avoid the jerk experienced by the user i.e. working against the magnetic forces in a cost effective way.

The different solutions provided by the different refrigerator manufactures which consists of the manual door handle based on lever 1^{st} class action, geared motor actuated push plunger and application of electromagnets to generate repelling force with the help of permanent magnets. The mechanical gain obtained from the lever 1^{st} class action is the function of the input and output link length that restricts its application in the constrained spaces and the concepts, which are based upon the electromagnets, requires large amount of current to work. Moreover, its manufacturing is not very cost effective. In case of the geared motor actuated push plunger, the push plunger is cost effective and is an automatic robust system. However, the number of parts are more as switches and sensors are required to detect the position of plunger and the additional component is required to change the polarity of motor to obtain the back and forth movement

of the plunger.

With an aim of jerk free door opening experience there is a need to provide a solution to avoid the jerk occurred due to magnetic force of attraction, this work is also very important from customer's view point, as it provides the convenience and satisfaction to the consumer while adding value to the product in cost effective way. It helps to build the consumer's good faith and perspective towards the refrigerator manufacturer. It also helps older, aged and physically disabled consumers. In future, it can be integrated with machine to machine interaction for automatic loading and unloading of food in refrigerator. It can be seen as robotic loading machine interface with refrigerator to automatically load the food in the refrigerator without any human interference, whenever robots interact with refrigerator it can automatically opens the door.

1.2 DIFFERENT METHODS TO SOLVE ENGINEERING PROBLEM

Engineering Problems solved by using following methods

a) Analytical method
b) Numerical method
c) Experimental method

ANALYTICAL METHOD

The solution of an engineering problem can be achieved through different approaches. In the mathematical treatment of an engineering problem, the physical system is converted into an equivalent mathematical system. Further, the solution of the mathematical system is obtained and correlated with the real engineering system. The solution of the yielded mathematical system may be obtained analytically or numerically depending upon the complexities involved with the system. The analytical method is a classical approach to solve a problem, the result provided by it is most accurate since there are no assumptions considered. However, they are applicable to limited problems as the exact solution can be solved for simple problem's governing equations. Whereas the numerical methods provide approximate solutions since certain assumptions are made while solving the governing equations. Due to advancements in computations, the analytical and numerical solutions may be achieved through modelling and simulations. Apart from mathematical modeling the engineering problem, the real engineering system or model is fabricated and the solution is obtained in the real time experimentally. In experimental method, the actual measurements are made to solve the problem. However, it is applicable only if physical prototype is present to perform the experimental studies and it is the

most time consuming method. Numbers of the experimental readings are taken to compensate the setup errors and other kind of errors. The basic procedure for solving any problem using the Analytical or Numerical approach is as follows:

1. Formulating a mathematical system from a physical system
2. Write the governing equation: The engineering principles associated with the physical systems are considered.
3. Solution of the governing equation mathematically. In case of numerical method, first assumption/boundary condition are considers and then they are solved using mathematical approximation method.

NUMERICAL METHODS

a) Finite Element Method (FEM)
b) Boundary Element Method (BEM)
c) Finite Volume Method (FVM)
d) Finite Difference Method (FDM)

Finite Element Method (FEM):

Finite element method is a numerical method to solve the variety of engineering problems approximately. The linear, nonlinear, buckling, thermal, dynamic and fatigue analysis can be performed using the FEM. The FEM is a versatile tool and widely implemented for the solution of engineering problems in commercially available software such as ANSYS, ABAQUS, COMSOL, etc. In the framework of FEM, the component or structure is discretized in large number of elements. The field variables are identified at specific locations called nodes of the element.

Boundary Element Method (BEM):

Boundary element method is useful to solve acoustics or noise and vibration (NV) problems. Similar to the finite element method, it also requires nodes and elements. However, it considers only outer boundary of the domain. Therefore, in this case if the problem is of volume, only outer surfaces are considered. If the domain is area then only outer periphery is considered. Thus, it reduces the dimensionality of the problem by a degree of one and thus solving it faster.

Finite Volume Method (FVM):

All computational fluid dynamics (CFD) software are based upon FVM. Unit volume is œnsidered in finite volume method. Variable properties at nodes are pressure, velocity, area,

mass etc. It is based on Navier – strokes equation.

Finite Difference Method (FDM):

Finite element and finite difference method share many common things. In general finite difference method is described as a way to solve the differential equations. It uses Taylor's series to convert differential equations to algebraic equations. It is used in combination of BEM or otherwise FVM to solve thermal and CFD coupled problems.

It should be noted that the FEM, being the most versatile method is used in the present work.

1.3 MULTI-BODY SYSTEM

Multi Body System can be defined as the assembly of different components acting in pre-defined manner due to action of forces and the joints interconnecting two or more bodies which constraint their motion. Forces can be identified as the contact, inertial, impact, gravity, friction and externally applied forces. In this context, the term multi-body is used to represent the complex systems encountered in a wide variety of industries such as transportation (automobiles, busses, trucks, trains, and planes), industrial machinery (textile, packaging, and manufacturing), aerospace systems (spacecraft and missiles), consumer goods (washing machines and watches) and electro-mechanical systems (printers and copiers). The mechanical system can be comprised of the rigid and flexible bodies connected by different kinds of kinematic constraints and flexible connectors. Multi body simulation is used in many engineering problems which may include:

- Evaluating the handling characteristics of an automobile while maneuvering on a road.
- Studying the force on knee or spine when humans perform an action.
- Evaluating the fatigue life of a machine component under action of loads
- Evaluating the stability of a flexible bodies subjected to External forces

1.3 MULTIBODY SYSTEM KINEMATIC AND DYNAMIC ANALYSIS

The two type of analysis which can be done while dealing with the study of multi-body system/assembly in motion are kinematic and dynamic analysis. The study of system's motion independently of the forces interacting with or within the system comes under the kinematic analysis resulting in the determination of position, velocity and acceleration of the system components. Only the interactions between system's components and the motions of system and its components are analyzed and simulated in kinematic analysis. As the interactions

between the forces and the motion of system are neglected, the motion of system is precisely specified, which is required to define the other kinematic characteristics of driving elements which calculates kinematic characters of other components based upon kinematic constrains equations. These kinematic characters describe the system topology.

The dynamic analysis of multi-body systems focuses on the understanding of the relationship between the motions of the system parts and cause of the motion due to interaction of external forces and moments. In general, the motion of the system is not prescribes; its calculation is one of the principal objectives of the analysis. The simulation of the external forces, which depends upon the relative position of the components of assembly such as forces exerted by actuator, dampers and springs, can be done in dynamic analysis. It is also possible to simulate the forces, which arise due to the interaction between the different components of system and their surrounding environments e.g. contact, impact, and frictional forces acting between two bodies. The reaction forces and moment generated at the kinematic joints constraints are also simulated from dynamic analysis. The reaction forces and moments restrict the relative motions between two or more connected bodies in prescribed direction.

Degree Of Freedom

The degree of freedom defines the number of possibilities for independent kinematical movements. Normally a rigid body has six degree of freedom three translational and three rotational. When the motion of a body is confined in the plane, then it has three degree of freedom one rotational and two translational. Degree of freedom(n) according to Kutzbach Criterion for planer kinematic mechanism defined as,

$$n = 3(l - 1) - 2j - h \tag{1.1}$$

Where, l is number of link, j is number of lower pair and h is number of higher pair.

Similarly, for 3-D mechanism the degree of freedom can be defined as

$$n = 3 * number\ of\ active\ links - number\ of\ constraints \tag{1.2}$$

Kinematic Constraints

The kinematic constrains restrict the one or more degree of freedom of a moving body or link. Different kinematic joints constraint the relative motion between kinematic links e.g. the revolute joint in planar motion restricts two translation motions which result in degree of

freedom equal to one while the translation joint restricts the one rotation and one translation motion resulting in the degree of freedom equal to one. However, the joints like cylindrical joint restrict only four degree of freedom as it allow only one rational and one translation motion of body.

Dependent and Independent Coordinates

The mathematical modeling of multi-body system requires a reference coordinate to define the position and motion. The number of coordinate systems required to describe the motion of system is equal to the number degree of freedom of motion. There are two type of coordinate system:

1. Independent Coordinate System
2. Dependent Coordinate System

Independent coordinate system directly defines the position of the bodies or the externally driven coordinates system, not the position of whole system Where as the dependent coordinate system can determine the position of all bodies in the system. Further the dependent coordinate system can be divided into two types which are:-

a) Absolute Dependent Coordinate System- defines the location of each element in relation to a fixed reference frame.
b) Relative Dependent Coordinate System- defines the location of each element with respect to the previous element of the kinematic chain.

Equation of Motion of Multi-body System

A multi-body system consists of a set of different interconnected rigid bodies, which undergoes displacement and rotations. The motion of n^{th} body in global coordinate system ($x_{n'}$-$y_{n'}$) is obtained by specifying a fixed reference frame (x_n-y_n) on each rigid body. The location of the nth body in the system can be obtained by specifying the origin of corresponding rigid body with respect to fixed coordinate system. The location can be expressed as:-

$$q_n = [x, y, \emptyset]_n^T \tag{1.3}$$

In equation (1.1), $\emptyset$ represents the relative angle between the global coordinate system and n^{th} body's fixed reference frame, also known as orientation of body in global frame. So, to define the location and orientation for the set of bodies in multi-body system in generalized coordinate system, the location can be written as:-

$$q = \{[x, y, \emptyset]_1^T, [x, y, \emptyset]_2^T, [x, y, \emptyset]_3^T \dots [x, y, \emptyset]_n^T \quad (1.4)$$

These bodies in a multi-body system are interconnected with each other by joints which restrict their relative motion or degree of freedom, as bodies in generalized coordinates are dependents on the each other. Such conditions can expressed as algebraic equations in terms of the generalized coordinate and time, which are also known as holonomic kinematic constraints:-

$$\varphi(q, t) = 0 \quad (1.5)$$

Assuming that the multi-body system is properly constrained and the number of constraints is equal to the generalized coordinates, than above equation can be used to derive the position 'q' of system components at any given time. From the position of component, the velocity and acceleration of all components can also be determined:-

$$\varphi_q \dot{q} = -\varphi_t \quad (1.6)$$

$$\varphi_q \ddot{q} = -(\varphi_q \dot{q})_q - 2\varphi_{qt} q - \dot{\varphi_{tt}} = \gamma \quad (1.7)$$

The velocity and acceleration are obtained by differentiating the equation with respect to time. The solution obtained from the above equation (1.7) determines the motion characteristics of constrained system which is referred as kinematic analysis.

In order to simulate system response under the action of the externally applied loads, it is necessary to employ the dynamic analysis, which requires the multi-body system assembly and solution of above differential equation of motion. Therefore, the dynamic equation of motion for system can be written as :

$$M\ddot{q} + \varphi_q^T \delta = Q^A \quad (1.8)$$

Where, M represent the mass matrix (mass and moment inertia system components), $\ddot{q}$ and φ_q^T represents the acceleration and Jacobian of the constraints of system respectively, δ is a Lagrange multiplier vector and Q^A is vector representation of external force applied. When the fixed coordinates of body lies on the centre of mass of the respective body, it significantly simplifies the general form of equation of motion. The reaction forces generated within the system are equal to the product of Jacobian vector and Lagrange multiplier. In case of an unconstrained system, the vector of Lagrange multiplier vector become null vector, therefore the above equation(1.8) is reduced to :-

$$M\ddot{q} = Q^A \tag{1.9}$$

The last two equations can be combined as the mixed system differential algebraic equation of motion, which can be expressed as:-

$$\begin{bmatrix} M & \varphi_q^T \\ \varphi_q & 0 \end{bmatrix} \begin{bmatrix} \ddot{q} \\ \delta \end{bmatrix} = \begin{bmatrix} Q^A \\ \gamma \end{bmatrix} \tag{1.10}$$

The dynamic response of the system can be obtained by solving the above equation. The solution procedure of above equation is summarized in the flow chart given below.

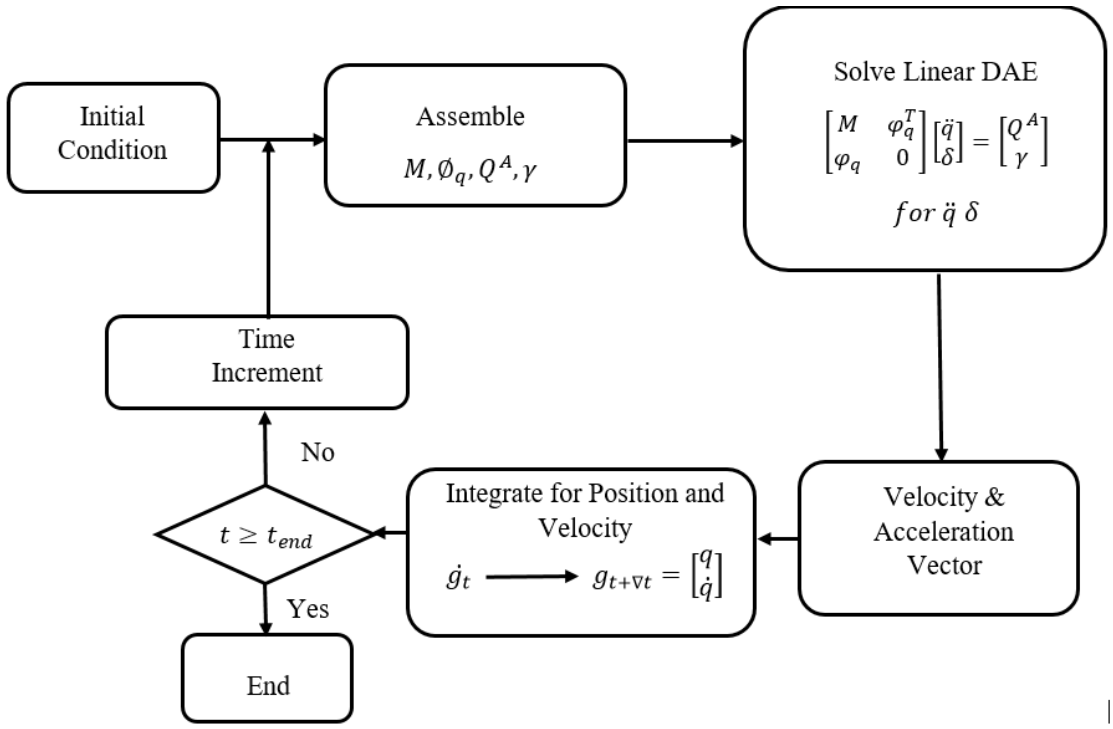

Figure 1.1: Integration procedure for the Differential Algebraic Equation

1.4 GENETIC ALGORITHM OPTIMIZATION

Genetic Algorithm (GA) is an evolution-based search algorithm used to solve complex multiple constraint or unconstrained optimization problems based upon the principle of natural selection which is derived from the biological evolution. In genetic algorithm, the population of individual solution modifies repeatedly. In each step, the parents are selected randomly from the individuals available in the population set and next generation children are obtained from the mating of the selected parents. The successive generations evolve the population toward an optimal solution. Problems which cannot be optimized by standard optimization technique and the non differentiable problem, discontinuous function, stochastic and non linear problems can also solved by using this technique. The problems with different mixed integer programmed

can be solved, where components are restricted to be integer valued. The GA is favorable for optimization of most real world optimization problems involving complexities like discrete, continuous or mixed variables, multiple conflicting objectives, non-linearity, discontinuity and non-convex region.

Principle of genetic algorithm

The basic principle of genetic algorithm, derived from biological evolution process, aims to solve the complex problems. The solutions for genetic algorithm are defined as the chromosomes group, expressed in the form of binary or float codes. Genetic algorithm initiate by generating an initial population randomly containing the number of hypothetical solution known as chromosomes. These hypothetical solutions are exposed to the environment (conditions for optimization) and the fittest chromosome will survive. The chromosomes which are more adaptive to the condition will be retained, crossed and divided to generate new generation of population involving a group of new chromosomes. In the search of the fittest function, according to the defined objective function the solution evolves to adapt to the environment, resulting in the optimized solution which is continuously evolving for several generations. There are three main operations for genetic algorithm to create the successive generation from the current population.

1) Selection

In selection operation, the individuals/parents are selected from the current population which are more adaptive to the environment/objective function. These selected individuals are chosen to form the population in next generation, which is known as regeneration or reproduction process. Roulette wheel selection method is used to decide which individuals shall breed to produce next generation population. According to Roulette selection criteria, the individual with higher probability of fitness value are inherited to next generation more than those individuals with lower probability of fitness value. The probability of each individual selected can be defined as follow:

$$P_i = {f_i}\Big/{\sum_{i=1}^{n} f_i} \tag{1.11}$$

Where $P_i$is the probability of number i individual to be selected,n is the group size,f_i is the value of fitness function for ith individual.

2) Crossover

In crossover operation, the genes from two chosen individuals interchange at the same place to generate a new individual. To generate a new individual, arithmetic crossover method is applied. The exchange of information in this process is random and aims to generate individuals with new combination of genes. The crossover probability decides weather the individual is involved in crossover or not. Generally the crossover probability value is kept in between 0.25 and 0.75. The different types of crossover techniques used in genetic algorithms are (a) one-point crossover (b) two point crossover (c) uniform cross over (d) ordered crossover (e) partial crossover (f) cycle crossover

a) One-Point Crossover

In one-point crossover, the two parents breed into two children. The two selected parents/individuals genes are exchanged over a randomly selected crossover point as shown in figure 1.2 below. The child 1 takes the genes from both of the parents, the genes of parent 1 on left side of the crossover point and the genes of parent 2 on right side of the crossover point. Similarly, the child 2 takes the genes of parent 1 on the right side of crossover point and genes on left side of crossover point of parent 2.

Parent 1	***1***	0	1	1	1	0	1
Parent 2	1	1	0	0	1	1	0
Child 1	1	0	0	0	1	1	0
Child 2	1	1	1	1	1	0	1

Figure 1.2: One Point Crossover

b) Two Point Crossover

Two point crossover is similar to the one point crossover but two crossover points are selected randomly. Then, the extreme segment of genes are swapped with each other to form the children as shown below in figure 1.3. It is also be possible to select n random crossover point. For example, the two crossover points selected after second and fourth place resulting in three segments and then the middle segment interchange with each other to produce the off spring.

Parent 1	***1***	0	1	1	1	0	1
Parent 2	1	1	0	0	1	1	**0**

Child 1	1	0	0	0	1	0	1
Child 2	1	1	1	1	1	1	0

Figure 1.3: Two Crossover

c) Uniform Crossover

In uniform crossover method, a template is created with random bits, the children receive their bits from parents as per the template shown in figure. As per the figure, Child 1 receives its bits from the parent 1 decided by templates, if template value is 1 than that bit from parent 1 is carried by off spring Child 1 and when template value is zero than it comes from parent 2. Similarly, Child 2 receives its bit from parent 1 if the template value for corresponding bit is zero and one form parent 2 if the corresponding template bit is one.

Parent 1	1	0	1	1	1	0	1
Parent 2	1	1	0	0	1	1	0
Template	0	1	1	0	0	1	0

Child 1	1	0	1	0	1	0	0
Child 2	1	1	0	1	1	1	1

Figure 1.4: Uniform Crossover

d) Ordered crossover

In some cases, while doing the crossover, there is either a loss of some solutions from the sets or duplicate solutions get created in the evolution process, such cases can be avoided by using the ordered crossover. Two parents are selected and a template created with random bits. Child 1 bits fills by the bits of parent 1 in segment with template bits value 1 the remaining bits of parent 1 are sorted with template bits value zero, the sorted genes bits appear in the same order as in parent 2 and they fill up the empty spaces let in Child 1. In similar fashion child 2 is created.

Parent 1	A	B	C	D	E	F	G
Parent 2	E	B	D	C	F	G	A
Template	0	1	1	0	0	1	0

Child 1	E	B	C	D	G	F	A
Child 2	A	B	D	C	E	G	F

Figure 1.5: Ordered Crossover

e) Partial Crossover

Partial crossover is similar to the order-based crossover, in it for given two parents, A and B, two crossover points are chosen. The genes between the cross over site are selected and the genes lying in the crossover site are swapped from one parent to another parent. For example, 5 in parent A is swapped with 2 of parent B similarly 6 is swapped with 3 and 7 is swapped with 10.

Parent A	9	8	4	5	6	7	1	3	2	10
Parent B	8	7	1	2	3	10	9	5	4	6

Parent A	9	8	4	2	3	10	1	6	5	7
Parent B	8	10	1	5	6	7	9	2	4	3

Figure 1.6: Partial Crossover

f) Cycle Crossover

In cycle crossover, initially some bits positions are fixed, the bits at these positions are inherited from parent 1 and bits at the non-fixed positions are interchanged with the respective parent 2 bits at that position to create the off spring.

Parent A	9	8	2	1	7	4	5	10	6	3
Parent B	1	2	3	4	5	6	7	8	9	10

Parent A	9			1		4			6	

Child A	9	2	3	1	5	4	7	8	6	10
Child B	1	8	2	4	7	6	5	10	9	3

Figure 1.7: Cycle Crossover

3) Mutation

Mutation operation is only for the selected individuals in which some genes of the selected individual are converted randomly to form a new individual. For example, the binary coded individuals during the mutation, bits 0 converted to 1 and vice versa. The mutation probability P_m decide the participation of an individual in mutation, generally P_m value is kept in between the range of 0.01 to 0.2.

Summary

In this chapter, a brief description of the design requirements of door handles of the refrigerators is discussed. Further, a general approach to analyses an engineering problem is described. It is noted that the finite element method is a versatile tool for solving engineering problems. The basics of kinematics are discussed in brief followed by the algorithm of optimization.

CHAPTER 2 LITERATURE REVIEW

This chapter presents the review of the work done in design of spur gear, compound gearbox under the space constrain, analysis of the door handle and kinematic and dynamic analysis of mechanisms employed in the different applications of mechanical engineering.

Balli and Chan (2002) studied the role of transmission angle in different mechanisms with 4, 5, 6 and 7 bar linkages. Transmission angle is the basis to compare effective force transmission capacity of the mechanisms. For four bar linkage mechanism, no motion and no torque can be transmitted to output link when the mechanism is at its dead center position i.e. transmission angle is 0^{o}. Low fluctuation in torque cannot be guaranteed when transmission angle is large and very large. The small transmission angle causes the errors in motion, unacceptable and noisy mechanism. The reduction in effective force transmission of four bar linkage mechanism can be noticed as the transmission angle deviates from 90^{o}, so to optimize the mechanism the linkage must be designed to minimize the deviation. In case of contact and trammel mechanism the transmission angle is kept constant. To design the mechanism with minimum coupler and bearing force, the transmission angle for the mechanism is kept maximum. It also affects the other parameters of mechanisms like mechanical advantage, input crank angle, pressure angle, force transmission, velocity, acceleration and friction. Pressure and transmission angle are complimentary angles. As the transmission angle deviates from 90^{o}, the frictional force also increases. Mechanical advantage is directly proportional to the sin of transmission angle. There may be one and more than one transmission angles possible for the five, six and seven bar linkage mechanism to have a most optimized design.

Bauchau and Ju (2006) modeled the flexible multi-body dynamic analysis with friction and demonstrated an approach to increase the accuracy and versatility of unilateral contact model in multi-body assembly. The planar and spatial clearance joints configurations were developed which were used for the bodies where both contacts and clearance occurs. The relative distance between the bodies, in-joint and relative tangential velocity driving intermittent contact model and friction model respectively can be obtained from the kinematic analysis. The friction model developed by LuGre is used in this work as it has an advantage to eliminate any discontinuity related to the Coulomb's friction law. Different discretization for normal and friction contact were proposed in which the energy balance model was used for the former while the energy dissipation model was used for later. The combination of both energy balance and dissipation model was used for discretization. This made the problem a numerically nonlinear stable

process. The numerical simulation provided the realistic results of dynamic analysis for contact and friction force at a joint.

Yoo *et al*. (2006) studied the displacement of beam by using the dynamic analysis of flexible body. Numerical simulation and experimental studies were conducted to analyze the large displacement of beam considering the motion and the damping forces resistance. The excitation of the system is done by using the shaker and function generator in the experimental setup. The displacement of the beam was captured by high speed camera. Numerical simulation of free vibration was conducted with higher value of damping coefficient to achieve static equilibrium position and the initial boundary condition were used to reconstruct the beam configuration. The numerical simulation were obtained by combining the absolute nodal coordinates and hybrid coordinate formulation model. Numerical simulation results were very close to experimental observations from which it was concluded that the hybrid coordinate formulation is more reliable way to simulate large displacement flexible bodies in motion.

Xing guo *et al*. (2007) simulated the crankshaft as a flexible component of engine assembly in multi-body dynamic analysis. A flexible multi-body system dynamic analysis FEA method was used to study the stress generated. The real-time dynamic loading condition on crank shaft was recorded which is important input parameter for optimization of crankshaft design. The model consists of crankshaft, connecting rod and piston. The working boundary condition and constrains were applied in ADAMS dynamic analysis software. The mechanical behavior of crankshaft of engine assembly was simulated under the practical working condition close to physical prototype analysis with fewer hypotheses and higher precision as compared to commonly analysis with user input boundary condition.

Alias and Majid (2008) performed the topology optimization study on the wiper mechanism using MotionView. They introduced multi-body dynamic analysis methodology for Altair MotionView to simulate the wiper dynamics while the contact region with windshield glass and the wiper link was topologically optimized by using Optistruct. Initially kinematic and dynamic analysis were performed in MotionView followed by the generation of flexible body and rigid body constraints in the hypermesh in which mesh, rigid, load collector, contact surface and materials were assigned to the wiper and imported into the motionView. Further, the Optistruct solver was selected within it to simulate the maximum stress and displacement of wiper mechanism links. Then, the best possible shape of wiper bracket was analyzed using topology optimization. In this multi-body analysis, it was found that the weight of the optimized wiper

bracket design reduced by 22% of original design and the shape obtained is less complex to manufacture. The optimized wiper bracket design was rechecked by performing the multi-body dynamic analysis in MotionSolve with initial boundary conditions. The overall maximum stresses obtain from simulation were less as compared to material yield stress, although the value of stresses increases as compare to stress values resulting from initial design.

Vadhe and Dave (2008) performed multi-body dynamic analysis on earthmoving equipment arm using MotionView. The earthmoving equipment was assembled in MotionView followed by automatically generating the meshed model and the joint. The boundary conditions were applied to simulate the model under the real conditions. Multi-body simulation was simulated by applying the cylindrical forces and motion to the hydraulic actuator for the rigid body model. The boom link is flexible body model was assigned in the assembly in MotionView to determine the stress in it. The model is simulated for two cycles of digging and dumping operations to determine the reaction force and stress generated in the flexible body. To investigate the stresses under the severe conditions occurs on critical location of Boom Link of excavator. The input parameters for the simulation were the mesh model of upper frame, lower frame, cabin, excavator cabin swing motor rotational speed, hydraulic cylindrical actuator's stroke length, speed and force for the cycle of digging and dumping. The output parameters were the reaction forces at each joints and the stress levels at different positions. The path of bucket tooth tip was also traced.

Gologlu and Zeyveli (2009) purposed an automated approach for preliminary gear drive design based upon the genetic algorithm. The volume of the gear drive is taken as the fitness function while the static and dynamic properties were considered as objective function. The design constraints were contact stress, bending stress, and face width. Two stage spur gear drive was designed by using this technique The volume of gear drive found by genetic algorithm technique is very close to the standard design procedure for gear drive design. The volume obtained from the genetic algorithm is 0.96 to 0.98 time of the volume of the standard gear drive design. It was recommended that the selection of genetic algorithm parameters is crucial for obtaining the accurate result over the defined global range.

Woo et al (2009) investigates the new design of the dispenser lever assembly which is simple mechanical lever system lever under the repetitive stresses to improve its reliability. The simple force and moment balances use to analyzed the load acting during the dispensing process Failure analysis and accelerated life testing were used to decide the key control parameter

material and size and levels of mechanical dispenser lever. They tested the three different designs one without ribs and fillet, one with ribs only and one with fillets only. The failure of existing design is due to the missing and poorly calculated design parameters like fillets around hinge rib are absent and at front corners and the thickness of hinge is small, it found that it fails in field and accelerated life test in three round occur both in the front corners of the lever and at the hinge. These parameters are consider in the next designs and modified it based upon the accelerated life test results. In redesigned dispenser lever, the failure rate decreases to the 0.1% and predicted life of the component is 10 years as compared to 8.3 year for initial design.

Huang et al. (2011) studies the effect of design parameters of five point double toggle clamping mechanism newly developed for the injection molding machines clamping operation. This study investigates the effect of design parameter on speed profile of clamping/moving platen, the stroke length of clamping hydraulic cylinder and mold opening, force amplification and initial closing speed and mold closing angle consider on performance of clamping mechanism. The optimization of the mechanism's design parameters is obtained by using the genetic algorithm; optimized design outperforms the motion characteristics as compare to prior design. The design parameter consists of three link lengths and two angles which are the variables of objective function of genetic algorithm. After optimization the stroke length of cylinder increases from .987 to 1.007, initially mold closing angle changes from 20.6^{o} to 23.5^{o} and force amplification increased to 20.4 from 19.93. The slight changes in design parameter greatly influence the performance of five point double toggle clamping mechanism as the force of clamping hydraulic cylinder reduced as the result of reduction in speed ratio compared to corresponding values of prior design but change in stroke ratios of the mold opening to the clamping hydraulic cylinder much smaller.

Engin Tanik (2011) proposed the transmission angle formulation for the complaint slider crank mechanism. Compliant mechanisms are those in with some or all motion is obtained through the deflection of flexible members. In this work two theorems were purposed one states that transmission characteristic of a compliant and rigid crank slider mechanism is similar if the ratio of higher value spring constant to output force magnitude times coupler link length is less than 1% and second theorem states that when a partially compliant crank mechanism with a full rotating crank, than the extreme point positions of transmission angle with respect to input crank angle are same as the rigid link slider crank mechanism. The theoretical and experimental

values input torque at crank measured with respect to crank input cycle and transmission angle which are nearly same. It is observed that if transmission angle increase above the 25^o the experimental and theoretical values of torque are inconsistent. For example, when θ=90°, the experimental value is 2.5 times of theoretical value. Negative effects on input torque fluctuation observed for low transmission angle.

Golabia et al.(2014) purpose a method to select the design parameters for any number of stage gearbox design with constrain of minimum volume/weight of gearbox by using the genetic algorithmic optimization technique for solving the objective function within designed constrained function. In this study a general form objective function derived with constrains for minimum volume/weight of any n number stages gear box, but two and three stage gear trains have been considered and solved by using Matlab program to minimize the volume/weight of gear train. The input parameters used for designing the gearbox are power input, gear ratio and hardness of gears. The result obtained from the optimization program has been presented in the form of practical curves which can be used to calculate the necessary parameters of gearbox like number of stages, shaft diameter, face width and gear modules. The two and three stage gear trains are designed by using these result and compared with the previous publication the material volume obtained is less as compared to the previous design methodology (Gear train optimization based on minimum volume/weight design).

Sutar and Shirodkar (2015) conducts the kinematic and dynamic analysis of steering mechanism, boom lifting mechanism and lid mechanism using Motion View and Motion Solve modules of Altair Hyperworks. The main objective of study is to check feasibility of mechanisms and to extract the dynamic joint forces information to design the different components of mechanism. These mechanisms assembly consists of different type joints constraints like sliding, translation, revolute and ball joint constraints in assembly. The multi-body dynamic analysis is used to compute the quasi-static forces at joints to compare the analytical calculation and finite element analysis result. Finite element helps to check the feasibility of mechanism and optimum selection of the hydraulic cylinders based upon the forces values obtained at the sliding joints. The output results are post processed in HyperView and HyperGraph to compare with analytical calculations. As the mechanism is modeled in the form of links and joints, so it needed to define different properties like mass inertia, centre of gravity location and density correctly before simulations. From kinematic analysis of the steering mechanism Ackerman angles of inner and outer wheel vs non dimensional stroke

length of piston is plotted to confirm the motion feasibility of steering mechanism and compare the simulation and analytically calculation. From Dynamic analysis the ratio of lateral force to applied force at bush (translational joint) is obtained which further plotted against the non dimensional stroke length of piston from which it can be observed that value of lateral force is high and it may lead to leakage problem in hydraulic cylinder over a period of time .Similarly the ratio of reaction force to applied force is obtained in boom lifting and lid mechanism with to the non dimensional stroke length of piston ,the result obtained from multi-body dynamics ,finite element analysis and analytical analysis are very close to each other with the error rate less than 1%.

Park *et. al*.(2018) investigated the different linkages mechanism and found that the toggle linkage is more useful for the finger clamp unit and the design is optimized for larger clamping force without changing the output joint angle, the performance index is the ratio of input torque to the output torque when output angle is in range of 0^o to 1^o, simulation and experiments results verified the performance parameter of the linkages. The constraints consider in for this study are closed chained linkage mechanism, degree of freedom should be equal to one and require radial input force should be small. For optimization purpose global optimization technique is used also known as genetic algorithm. The output torque obtained as the function of output angle. The lengths of different links are considered as the optimization parameter in the genetic function.

CHAPTER 3 METHODOLOGY AND SIMULATION

3.1 PROBLEM DEFINITION

In refrigerator, both doors are equipped with magnetic gasket sealing to prevent the leakage of cold air from the inside of the refrigerator and freezer cabinet. The force of attraction between the magnetic gasket sealing and steel frame of refrigerator is in range of 60N to 80N, which is recorded experiment in running environment. The old users and the users with physical disability experience difficulties to produce 60-80N pull force, required to open the door. This causes internment jerky experience to user while opening the door as the amount of torque required to turn the door is equal friction torque required to overcome the friction torque of hinge.

In order to make the door opening experience more comfortable for the user, there is a need to provide mechanism in door handle that amplifies the input force at the expense of displacement to reduce the jerk. The new door opening mechanism should be designed with existing space and mounting constrains while keeping the cost and assembly time as minimum as possible. The allowable rotation displacement of lever handle should be kept less than 45^{o}.

From the past study of patents it is found that the mechanism used in door opening mechanisms are mechanical first class lever action mechanism, geared motor push plunger mechanism and electromagnetic push plunger actuators. From the past study and experience the mechanical mechanisms and the gear motor actuator are much effective as compared to electromagnetic actuator which requires more power to operate and the cost to manufacture is more as compared to other.

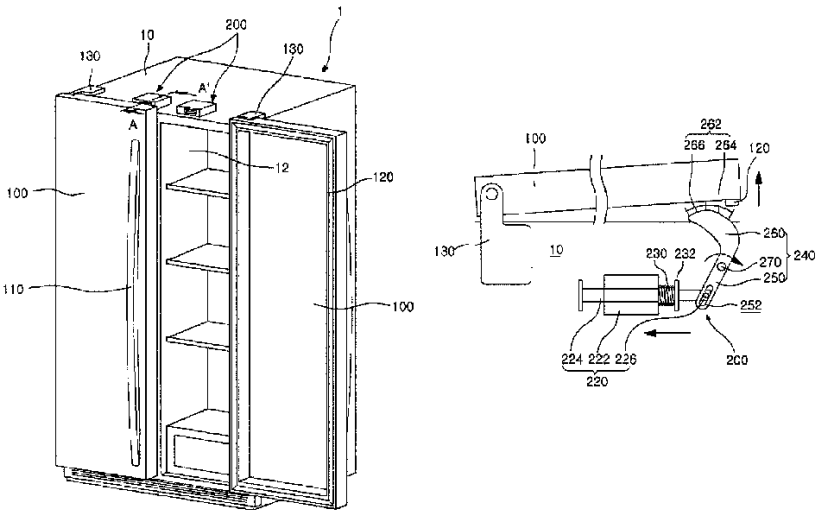

Figure 3.1: Patent No. US8444237B2 (2013) Filed by LG Uses the Solenoid with 1st Class Lever Action

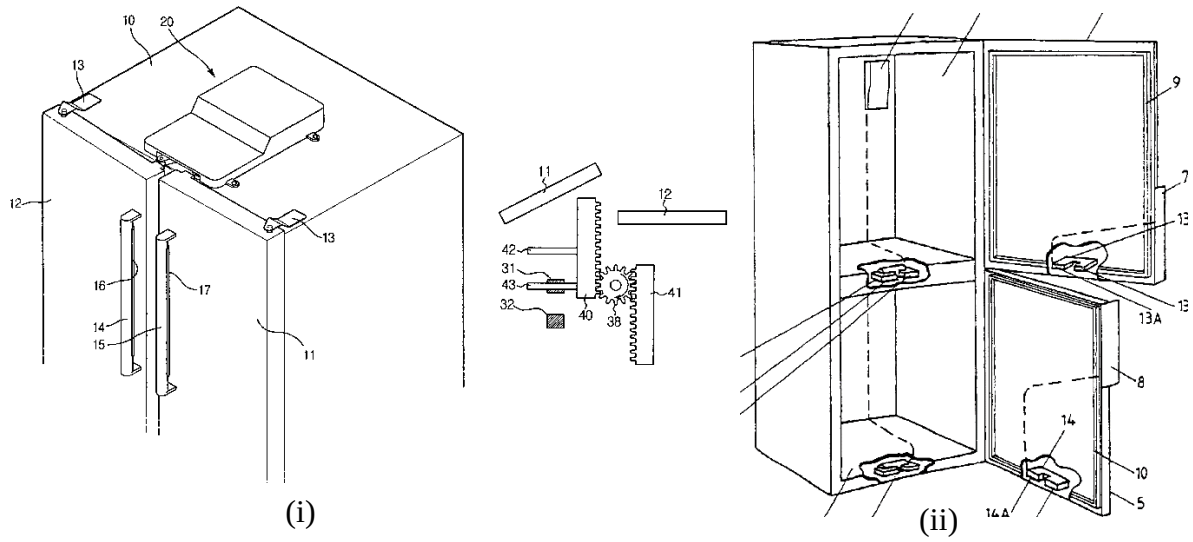

Figure 3.2: (i) Patent No. US8297725B2 (2012) Filed by Samsung Uses Geared Motor Actuator and (ii) Patent No. US6811236B1 (2004) Filed by Fisher & Paykel Appliances Ltd Uses Electromagnet with permanent Magnet

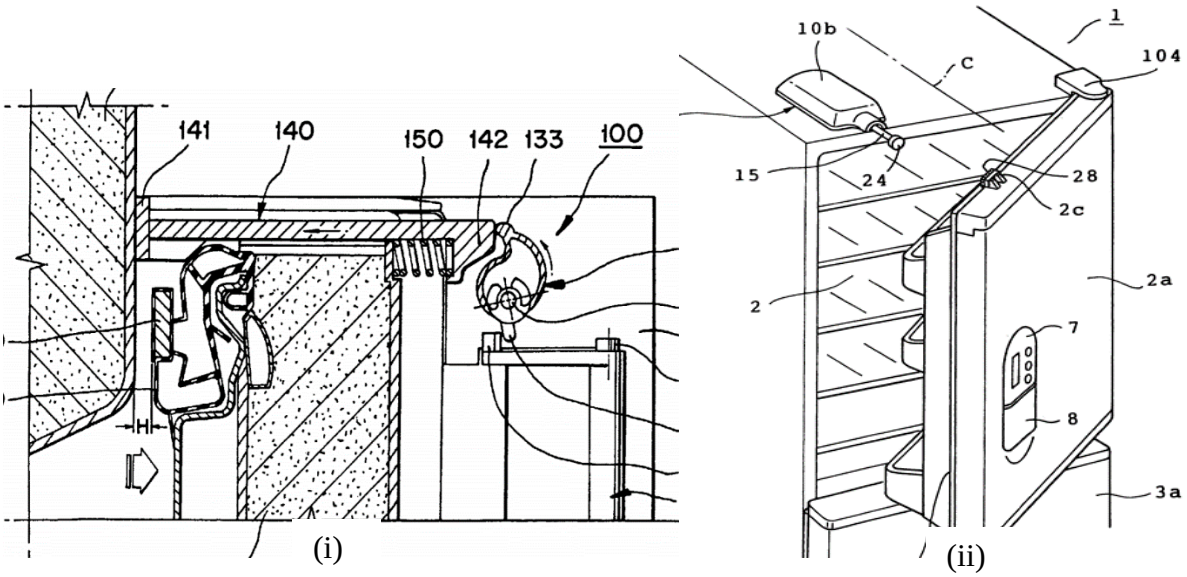

Figure 3.3: (i) Patent No. US005908228A (1999) Filed by Samsung Uses the 1st Class Lever Action and (ii) Patent No. US6338536B1 (2002) Filed by Toshiba Uses the Solenoid Actuator

In figure 3.1 Patent No. US8444237B2 uses the solenoid actuator with smaller actuation forces, which further magnified by using the first class lever action. This first class lever action is also used in Patent No. US005908228A, which is a manual handle it reduce the human effort required to open the refrigerator door. In Patent No. US6338536B1 use the principle of electromagnetism, in former patent working similar to the solenoid actuators in which the metal plunger is magnetically charge with opposite magnet pole with respect to induction coil winding and in Patent No. US6811236B1 the electromagnet and a permanent magnet combination is used to open the refrigerator door present on door, as the same magnet pole

repel each other. But in patent US8454102B2 and US8297725B2 a geared motor with a rack and pinion gear combination is employed to obtained push force required to open the refrigerator door.

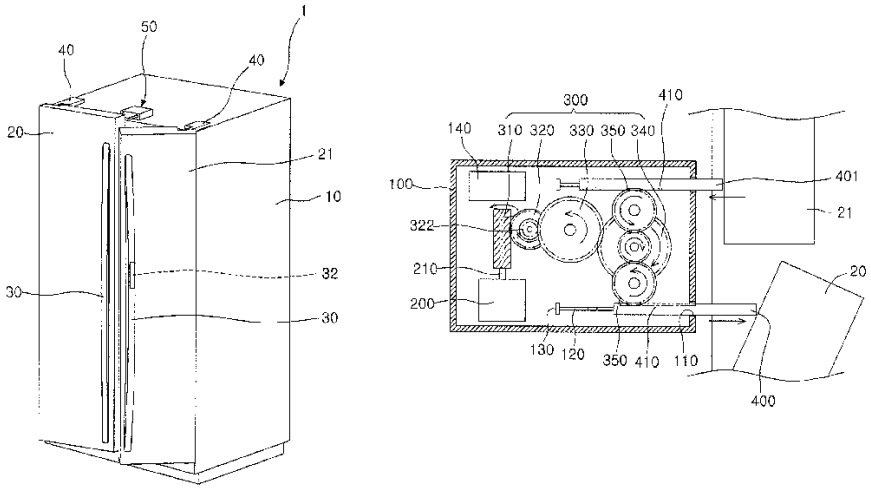

Figure 3.4 Patent No. US8454102B2 (2013) Filed by LG uses Geared Motor Actuator

The design and validation of the any mechanism is a crucial for design process of a complete module. The CAD and CAE tools help to speed up the design and analysis process, which reduce the time to market launch and reduce the production cost. The designed mechanism and its parts are validated by the kinematic and stress analysis by using the multi body dynamic simulation study under working environment, by using the virtual simulation CAE tools.

3.2 TOGGLE MECHANISM

Toggle linkage mechanism is basically a crank slider mechanism which is widely used in everyday life machines. The large output force can be generated with respect to a small input force applied to toggle linkage mechanism. Hence, it is particularly used for tasks that require large forces like press machine and clamping device. Main application can be found in earlier mechanical printing press machines, mechanical press machine, jigs, fixtures, plastic injection molding machines and rock crushing machines etc. It is not used in any kind of door handle or with the mechanical lever action handle because of its complex structure which is difficult to fit in the small packaging space like refrigerator door handles.

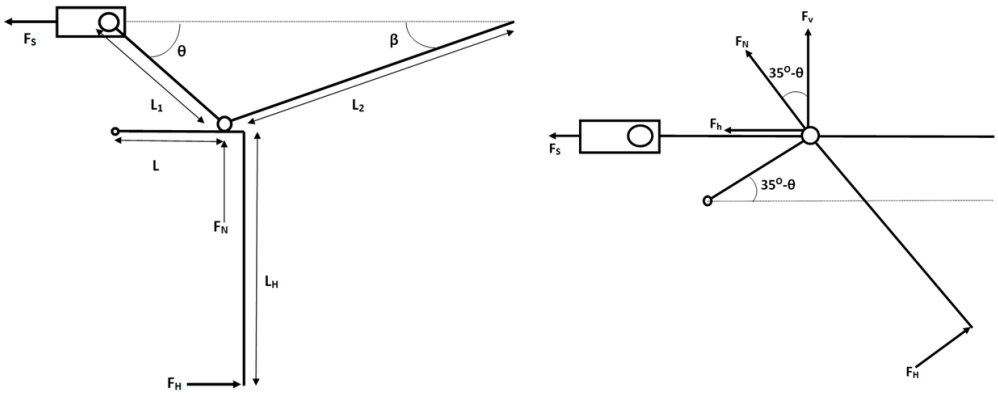

Figure 3.5: Block Diagram of Toggle Mechanism

L_H : Length of lever handle (Vertical distance between hinge point and force line of action)

L : Distance between hinge point and vertical push force (link L).

L_1 : Length of link 1

L_2 : Length of link 2

F_H : Pull force applied on lever handle

F_V : Vertical Push applied on joint of link 1 and link 2

F_S : Push Force on the slider

θ : Angle between link 1 and horizontal axis (initially θ is 35°)

β : Angle between link 2 and horizontal axis

γ : Angle between link L and horizontal axis

F_{SV} Vertical reaction force on the slide.

From the above Fig.4 the input force to the toggle mechanism at pin joint of link1 and link2 can obtained as,

$$F_N = \frac{F_H . L_H}{L - L_2(\cos(\sin^{-1}(\frac{L_1}{L_2}\sin\theta)) - \cos(\sin^{-1}(\frac{L_1}{L_2}\sin 35)))} \quad (2.1)$$

$$F_v = \frac{F_H . L_H . \cos(35 - \theta)}{L - L_2(\cos(\sin^{-1}(\frac{L_1}{L_2}\sin\theta)) - \cos(\sin^{-1}(\frac{L_1}{L_2}\sin 35)))} \quad (2.2)$$

From Fig 3.5 the free body diagram ,

$$F_1 \cos\theta + F_h = F_2 \cos\beta \quad (2.3)$$

$$F_1 sin\theta + F_2 sin\beta = F_v \quad (2.4)$$

From equation (2.3) we get,

$$F_2 = \frac{F_h + F_1 \cos\theta}{\cos\beta} \tag{2.5}$$

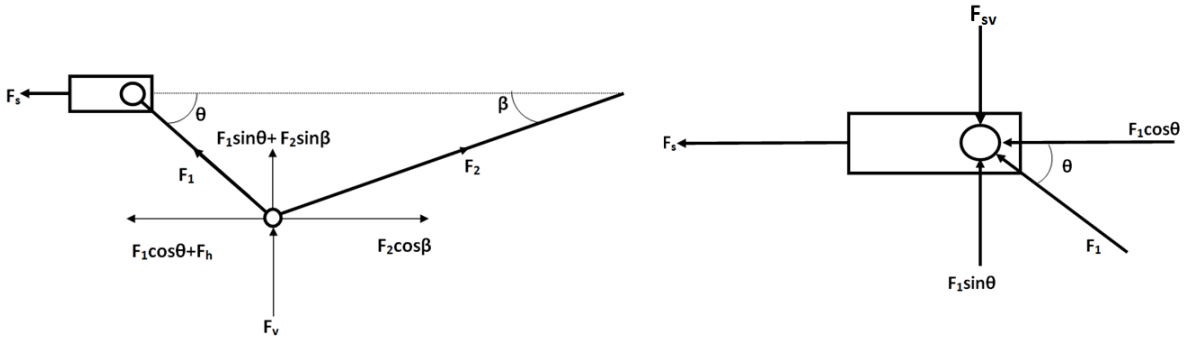

Figure 3.6: Free Body Diagram of Mechanism

Substituting the value of F_2 from equation (2.3) in equation (2.4),we get,

$$F_1 \sin\theta + \frac{F_h + F_1 \cos\theta}{\cos\beta}.\sin\beta = F_v \tag{2.6}$$

$$F_1 = \frac{F_v - F_h \tan\beta}{\cos\theta\,(\tan\theta + \tan\beta)} \tag{2.7}$$

$$F_s = F_1 cos\theta \tag{2.8}$$

$$F_s = \frac{F_v - F_h \tan\beta}{(\tan\theta + \tan\beta)} \tag{2.9}$$

$$F_s = \frac{F_H.L_H(\cos(35-\theta) - \tan\beta\,.\sin(35-\theta))}{\left(L + L_2\left(\cos\theta - \cos\left(\sin^{-1}(\frac{L_1}{L_2}\sin 35)\right)\right)\right)(\tan\theta + \tan\beta)} \tag{2.10}$$

Where, $\beta = \sin^{-1}(\frac{L_1}{L_2}\sin\theta)$

From above equation (2.10), the mechanical advantage (M) of whole mechanism can obtained as the ratio of push force on slider to pull force required to move the lever handle and the net stroke length (L_s) of the slider are given below:-

$$M = \frac{F_s}{F_H} = \frac{L_H(\cos(35-\theta) - \tan\beta\,.\sin(35-\theta))}{\left(L + L_2\left(\cos\theta - \cos\left(\sin^{-1}(\frac{L_1}{L_2}\sin 35)\right)\right)\right)(\tan\theta + \tan\beta)} \tag{2.11}$$

$$L_S = L_1 + L_2 - \left(L_1.\cos 35 + L_2.\cos\left(\sin^{-1}(\frac{L_1}{L_2}\sin 35)\right)\right) \tag{2.12}$$

Here value θ lie between 0° to 35°, L_H=120 mm and L=40 mm are predefined, but L_1 and L_2 are needed to be optimized for the maximization of mechanical advantage of whole mechanical

mechanism for the given space constrains.

From the equation (2.11) and (2.12), we investigates the effect of different linkage lengths on the mechanical advantage and stroke length, which are the main design parameters for designing the mechanism.

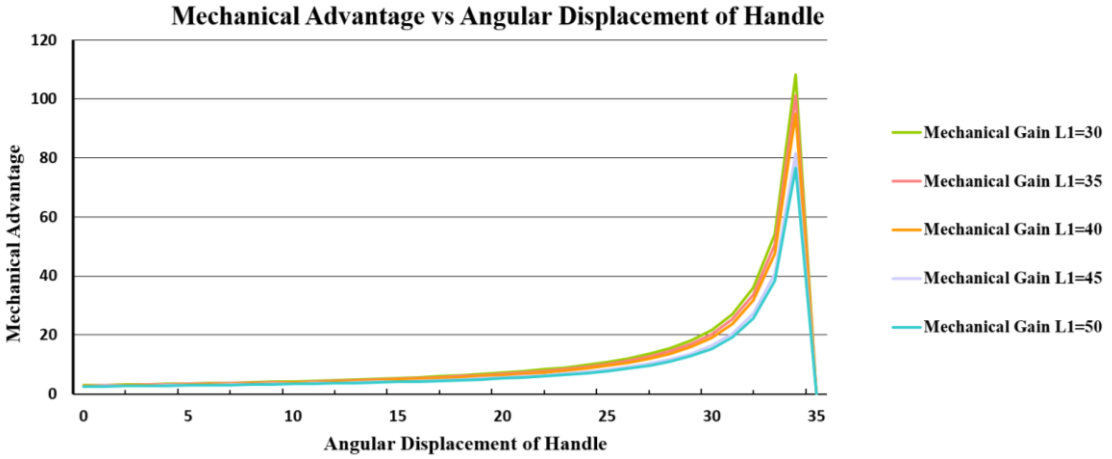

Figure 3.7: Mechanical Advantage vs. Door Handle Angular Movement (L_2=75 mm)

Case 1:-When Link 2 length is kept 75 mm and Link 1 length is varied in the range of 30 to 50 mm. In figure 3.7, it can be observed that initially when the angular displacement ranges from 0^o to 10^o the change in mechanical advantage is not significant for different length of link 1. A pattern can be observed between the length and mechanical advantage as the link with smaller length has higher value of mechanical advantage value as compared to longer links. In between the range of 15^o to 30^o the value of mechanical advantage increases with respect to the length of link 1.

From figure 3.8, it can be observed that the gap between the mechanical advantage profiles for different link 1 lengths start increases after the 20^o and all approaches to the peak value. Maximum peak value can observed for smallest length of link 1.

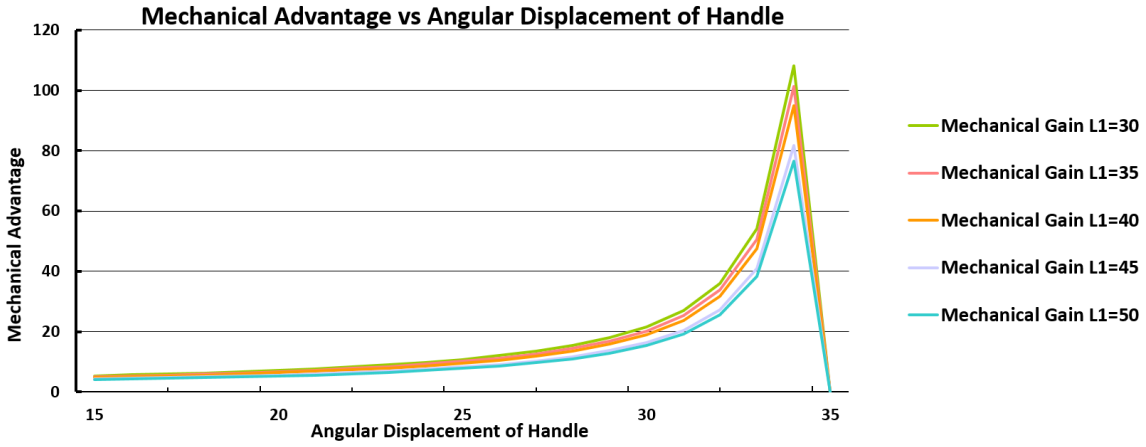

Figure 3.8: Mechanical Advantage vs. Door Handle Angular Movement between 0^o to 30^o (L_2=75 mm)

Figure 3.9 shows the displacement of the slider with respect to angular displacement of the handle. It can be observed that the net slider stroke length increases as the length of link1 increases, but it can be observed that when the length of link is longer, then it travels more distance as compared to the smaller links between the range of 25° to 35°. After 25°, the rate of displacement in slider with link starts decreasing which is the reason for smaller link possessing higher increase in mechanical advantage as compared to others.

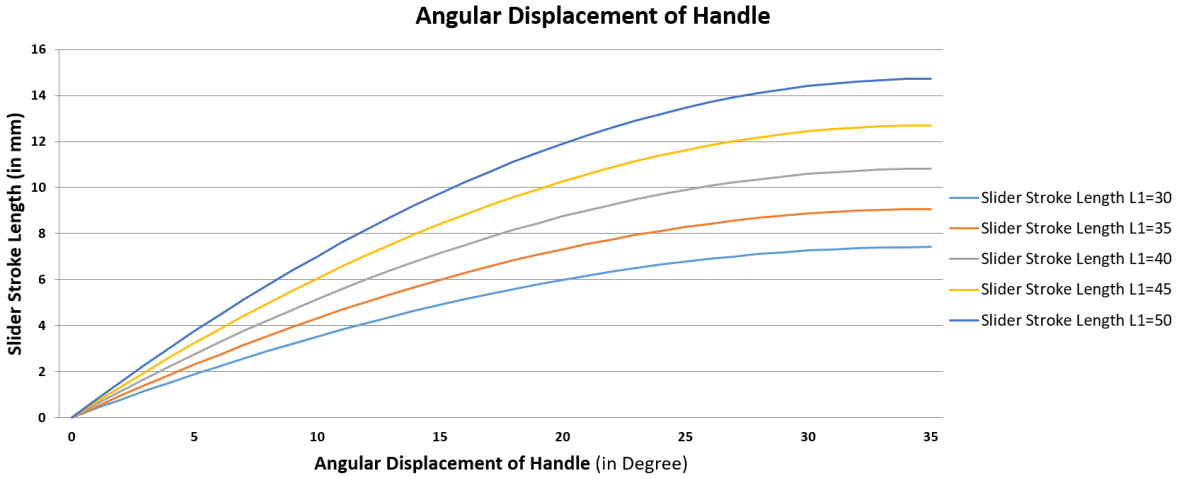

Figure 3.9: Slider Stroke Length vs. Door Handle Angular Movement (L_2=75 mm)

When link1 length is greater than 40mm, net displacement of the slider is approximately 10mm from angular movement between 0° to 25°. So, the effective working net displacement is 25°.

Case 2:-When Link 1 length is kept 40 mm and Link 2 length is varied in the range of 65 mm to 85 mm.

From figure 3.10, it can be observed that the curves of mechanical advantage of different link 2 length are much closer to each as compared to case 1. The difference between the mechanical advantage value is very small for a particular angular displacement for given different link2 lengths. It can be observed that longer link 2 has the higher peak value of mechanical advantage. The change patterns in mechanical advantages are observed between the ranges of 15° to 30° similar to case 1. The difference in the peak magnitude of mechanical advantage between two consecutive lengths is very small.

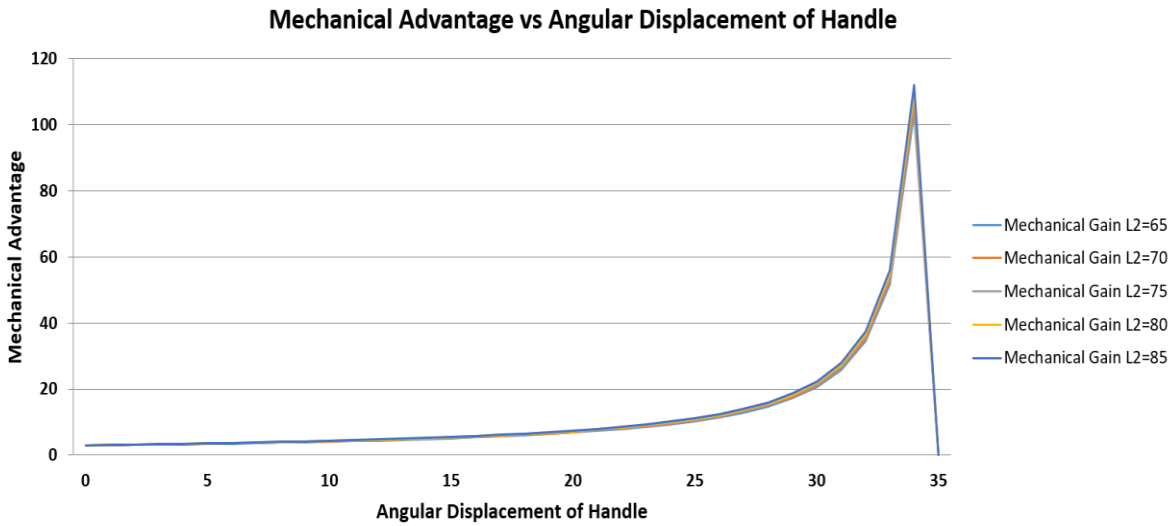

Figure 3.10: Mechanical Advantage vs. Door Handle Angular Movement (L_1=40 mm)

Figure 3.11 shows that the gap between values of mechanical advantage is smaller as compared to case 1 in between the range of 15^o to 30^o angular displacement as the curves of mechanical advantage for different lengths link 2 are closely aligned to each other.

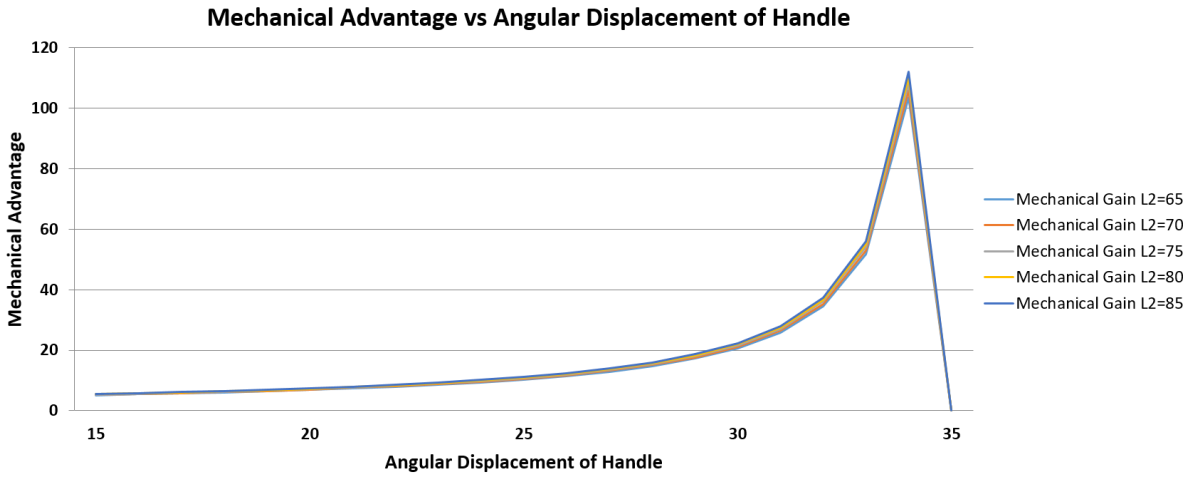

Figure 3.11: Mechanical Advantage vs. Door Handle Angular Movement between 15^o to 30^o (L_1=40 mm)

From figure 3.12, it can be observed that the net stroke increases as the length of link 2 increases. Until 25^o angular displacement, the stroke length change is approximately linear with respect to angular displacement. The net displacement is smaller in case of larger length of link L_2. Maximum net displacement is observed in the case L_2 =65 mm and the rate with which it increases with respect to angular displacement is also higher as compared to other cases, as the gap between curves start increasing non linearly. This explains the lesser magnitude of mechanical advantage in this case as compared to the other.

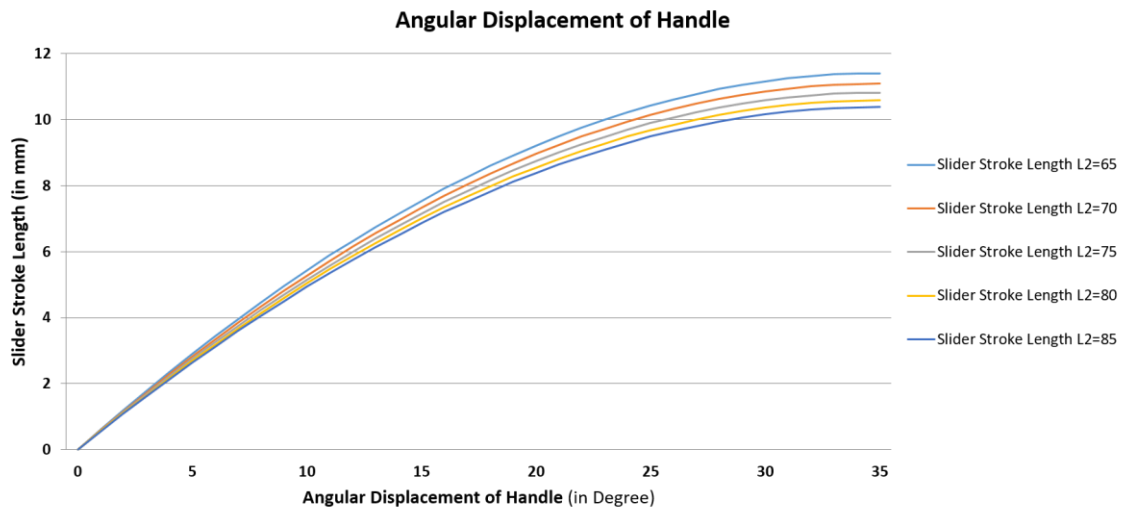

Figure 3.12: Slider Stroke Length vs. Door Handle Angular Movement (L_1=40 mm)

3.3 DESIGN CONSTRAINS

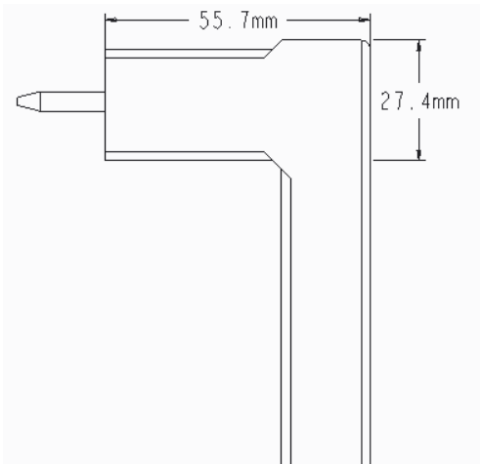

Figure 3.13: Existing Design Constrains

The aim of this study is to develop a toggle lever mechanism which produces maximum push force with minimum 10mm slider displacement. The Mechanical advantage force-amplification ratio of the output force to the input force is considered as performance indicator. The optimization of design parameter is to be done to maximize the performance indicator. The Genetic Algorithm is well known tool of optimization for determining the global maximum which is used to find the optimum values of lengths of both the links

3.4 DEFINING THE OBJECTIVE FUNCTION

Objective function is that quantity which has to be minimized or maximized by exploring a search domain under the given constraints. The objective function F_{obj} of this study is to maximize the magnitude of mechanical advantage and it is defined as:-

$$F_{Obj1} = Max\ M(L_1, L_2) \tag{2.13}$$

$$F_{Obj2} = Max\ L_{S30}(L_1, L_2) \tag{2.14}$$

Where M and L_{S30} are given as:

$$M = \frac{F_s}{F_H} = \frac{L_H(\cos(35-\theta) - \tan\beta\,.\sin(35-\theta))}{\left(L + L_2\left(\cos\theta - \cos\left(\sin^{-1}(\frac{L_1}{L_2}\sin 35)\right)\right)\right)(\tan\theta + \tan\beta)} \tag{2.15}$$

$$L_{S30} = L_1 + L_2 - \left(L_1.\cos 30 + L_2.\cos\left(\sin^{-1}(\frac{L_1}{L_2}\sin 30)\right)\right) \tag{2.16}$$

And the constraint functions are defined according to the given constraints of space. These constraints are mathematically expressed as:

$$L_1.\cos 35 \leq 35 \tag{2.17}$$

$$L_2.\sin.(\sin^{-1}(\frac{L_1}{L_2}\sin 35)) = L_1.\sin 35 \tag{2.18}$$

$$L_1 + L_2 - \left(L_1.\cos 35 + L_2.\cos\left(\sin^{-1}(\frac{L_1}{L_2}\sin 35)\right)\right) \leq 10 \tag{2.19}$$

$$L_1 \sin 35 \leq 22 \tag{2.20}$$

From the above equation, we obtain the optimum values of $L_1 = 40.102mm$ and $L_2 = 78.09mm$, the process of optimization is discuss in next section. The mechanism is designed by using the $L_1 = 40mm$ and $L_2 = 75mm$ for the ease of design. Instead of using complete link2 we provided a slot which traces the curve path followed by pin joint at one end of link2. This slot guides designed with minimum thickness of 2mm, to makes it strong enough to with stand the reaction forces.

3.4 OPTIMIZATION BY USING GENETIC ALGORITHM OPTIMIZATION APPROACH

In this section, MATLAB in built Genetic algorithm optimization toolbox is applied to obtained the optimized values of two link length which are the design parameters. It generates a new population of feasible solution for the provided problem in each cycle. Initially, a random population is created which represents the potential solution of given problems which are created to start search operation. The population elements are encoded into bit string known as chromosomes. The fitness value define the performance of the string, which is evaluated from the function under the defined constraints of the problem. Based upon the fitness function value, of chromosomes are selected, their selection influence the process of genetic manipulation. The selection process assures the survival of best fit individuals. The genetic manipulation process

is carried out after the selection process of the chromosomes. This manipulation process is carried out in two steps, one is crossover operation and the other is known as mutation. In crossover operation, the genes of two parent chromosomes are recombined to generate the off spring. In mutation process, the genes one or more are randomly selected and their positions are altered within the chromosomes. This next generation which are obtained from genetic manipulation were evaluated for the given constraints. For the execution of genetic algorithm, some parameter need to be specified initially, like population size, maximum no. of generation, mutation probability, fitness function, crossover probability, range of design variable etc. The procedure follow to execute the multi objective genetic algorithm is given below:-

STEP1. Define the objective function and constraint function. Specify the objective and constraint function as the mathematical modeled function of design variable such as length of links (L_1) and radius of slot (L_2), the range of design variables. The objective and constraints function for design problem are non linear and inequality in nature.

Objective Functions

$$F_{Obj1} = Max\ M(L_1, L_2) \tag{2.21}$$

$$F_{Obj2} = Max\ L_{S30}(L_1, L_2) \tag{2.22}$$

Constraint Functions

$$L_1.\cos 35 \leq 35 \tag{2.23}$$

$$L_2.\sin.(\sin^{-1}(\frac{L_1}{L_2}\sin 35)) = L_1.\sin 35 \tag{2.24}$$

$$L_1 + L_2 - \left(L_1.\cos 35 + L_2.\cos(\sin^{-1}(\frac{L_1}{L_2}\sin 35))\right) \leq 10 \tag{2.25}$$

$$L_1 \sin 35 \leq 22 \tag{2.26}$$

STEP 2. Initial population generation and goal function evaluation. The random binary population is generated which is be converted into the real number before evaluating the goal function. The double vector population type is selected with population size of 50, the non linear feasible population function is selected for initial population creation function.

STEP 3. Coding and Decoding. The most common encoding in genetic algorithm is binary in which every chromosome is string into 0 and 1 bits. This encoding is not suitable for many problems. While solving the problem with Genetic Algorithm, the each searching range is binary string code which enables the reproduction, mutation and crossover of chromosomes and then it again decoded into the real numbers to evaluate the goal function.

STEP 4. Reproduction Process. Tournament selection function is selected as reproduction method. The next generation is reproduced based upon the best parent obtained from the tournament between two parents.

STEP 5. Crossover. The two parent chromosomes which are selected randomly to reproduce the next generation by exchanging the genes with each other. The constraint dependent cross over function is selected with crossover rate of 0.8.

STEP 6 Mutation. In mutation operation the position of genes within the chromosomes are altered randomly or based upon the defined function. The mutation functions of type adaptive feasible is selected.

STEP 7 Termination rule. Genetic algorithm keeps on searching uninterrupted for solution for the goal function unless there is no stopping criterion is defined. To stop the calculation the goal function tolerance of $1x10^{-4}$ and constraint tolerance of $1x10^{-3}$ are defined

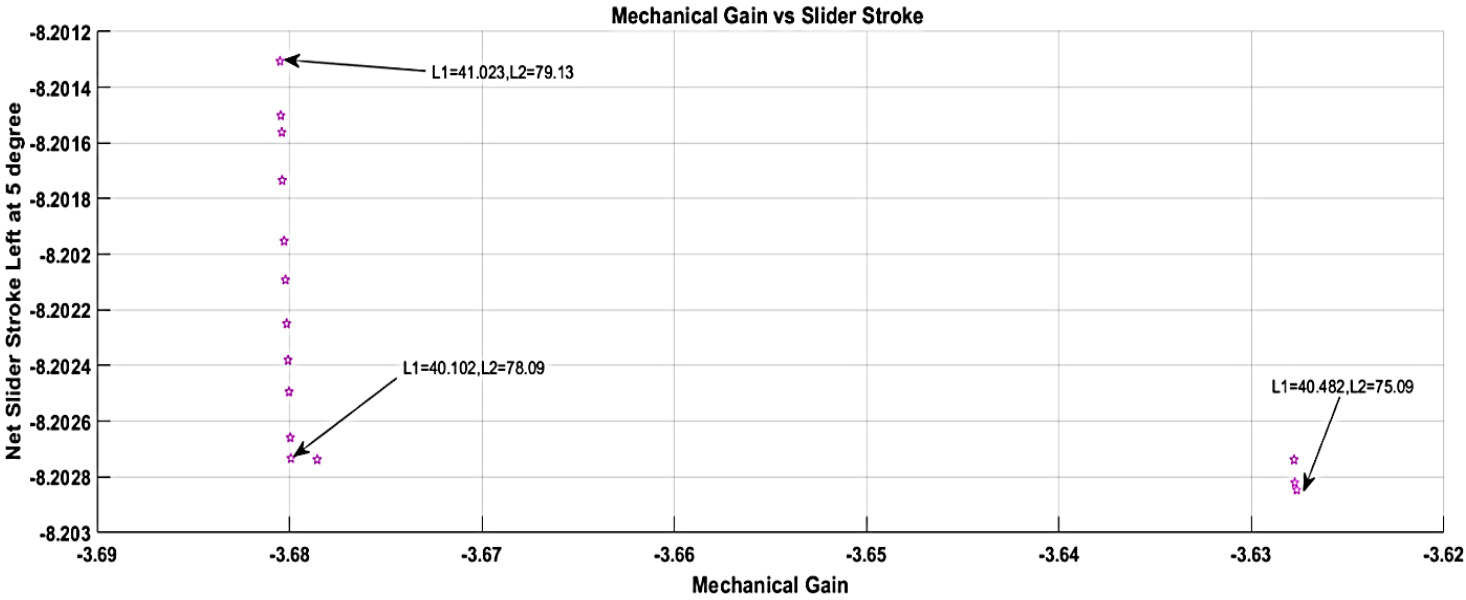

Figure 3.14: Genetic Algorithm Result for Maximization of Objective Function

The figure 3.14 shows the result of genetic algorithm which objective functions are minimized, but by multiplying the objective function with negative function, it becomes the problem of maximization. From above result, it is observed that when link length L_1=41.023 mm and slot radius L_2=79.13 mm, the mechanical gain is maximum and net stroke length of slider is minimum by very small amount but for link length L_1=40.482 mm and slot radius L_2=75.09 mm the mechanical gain is less than 3.63 and net stroke length of slider is maximum 8.2029. When L_1=40.102 and L_2=78.09, then the mechanical gain is less than 3.68 and net stroke length of slider is maximum 8.2027 which are large as compared to 40.482 mm and 75.09 mm. It should be noted that to keep the design within the design constraints, link length L_1=40.482

mm and slot radius L_2=75.09 are chosen. So, the link length equal to 40 mm and slot radius equal to 75 mm is selected for designing the refrigerator door handle.

3.5 DESIGN AND ANALYSIS OF DOOR OPENING ASSIST MECHANISM

The present section summarizes the details of background information of mechanism and kinematic analysis. The complete design and kinematic analysis cycle requires following steps (1) Design of Internal parts of mechanism, (2) Kinematic and dynamic analysis (i.e. multi-body simulation) and (3) Stress analysis. The major steps for designing mechanisms:

1) The layout design of all internal parts of door opening assist mechanism on the basis of packaging space and mounting position available on the refrigerator and selection of motors and dimension of parts based on the load calculations.
2) Based on the permissible rotational displacement angle of the handle and partition of magnetic sealing gasket the link length and slot dimension are finalized. In case, of geared motor actuator, the stroke length and push force decides the gear train designs.
3) Based upon above, different parameters of mechanism design are finalized.
4) Consumer ergonomic decides the width of holding portion of handle in mechanisms and dimensions of gears in geared motor actuator is decided by the loading conditions.
5) HyperWorks CAE tools are used in multi body simulations and analysis to validate the designs.

3.6 DESIGN OF THE DOOR HANDLE COMPONENTS

As door handle act as a lever its cross section is designed based on the bending stress induced due to the bending moment which is induced because of force applied at some distance from the hinge point. Initially the maximum force can be applied on the door handle is considered as 100 N. In working the action, the nature of force applied is sudden so the factor of safety is chosen as 2 and distance between the hinge and line of action of force is 120 mm. The cross section of the handle is elliptical with major axis of 32 mm and minor axis of 22 mm and the wall thickness is of 2 mm, so the moment of inertia for the handle cross section is 6933.12 mm^4 and the radius of curvature (R) is 10 mm. By using the bending moment equation, the bending stress are calculated in the handle is calculated.

$$\sigma_b = \frac{M.R}{I} \tag{2.27}$$

From above equation, the bending stress obtained is $\sigma_b = 34.69 N/mm^2$ which are less than allowable flexure strength of ABS is 74 Mpa, so it safe to design the handle with wall thickness of 2 mm. The ASB HG173 material mechanical properties are provide in the appendix. The

coupler link is designed under the compressive loading condition with the factor of safety 2. The maximum compressive load that can be applied on the coupler is equal to magnet force required to open the refrigerator door which is 100 N including effect pressure difference on door inner outer surface. Max compressive yield strength of ABS is 65 MPa and minimum cross section of a coupler is 25 mm^2, so the max compressive stress induce within coupler is 8 MPa which is safe for given area of cross section.

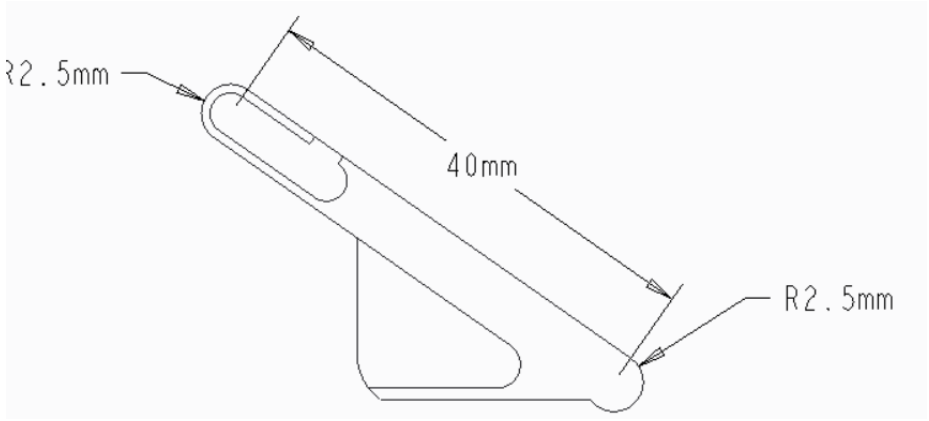

Figure 3.15: Design of Coupler

The pins present on the coupler as shown in Fig 3.15 can fails under the shear stress, the maximum force acting upon it can be written as

$$F_{pin} = \sqrt{P^2 + (m.P)^2 + 2.m.P.\cos\theta} \tag{2.27}$$

The diameter of the pin is 5 mm. The value F_{pin} obtained from above equation (2.27) is 60.231 N and which result in the shear stress of 6.138 MPa with factor of safety 2, which very is less as compare to permissible Shear for ABS is 23 MPa.

The last component slider design is a accomplished by considering it as a column structure which fails under critical buckling load can written as:

$$P_{cr} = \frac{\pi^2 EI}{K.L^2} \tag{2.28}$$

Where P_{cr} is maximum critical buckling load, E is Young's modulus (2.35GPa for ABS), I is moment of inertia and K=1. P_{cr} obtain from the above equation (2.28) is 188.0528 N and permissible load with factor of safety 2 it becomes 94.26 N which is greater than 66 N (standard refrigerator door opening force).

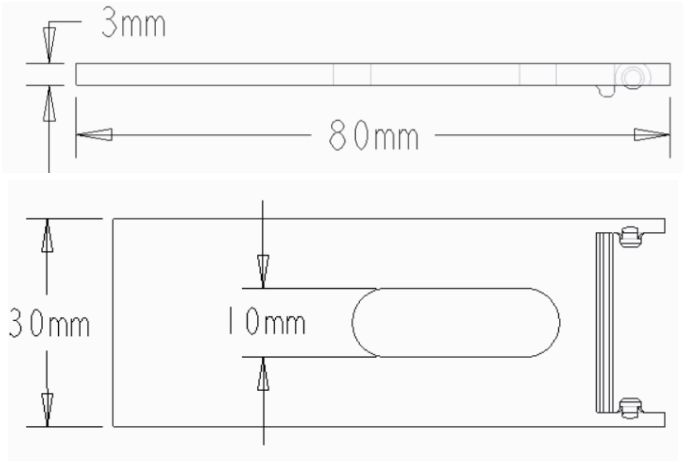

Figure 3.16: Slider Design

KINEMATIC ANALYSIS OF MECHANISMS

The kinematic analysis and the details of door handle mechanism are discussed in this section. The steps followed to conduct the kinematic analysis are create a motion view model, define inputs, create joints and 3D contact surfaces, conduct analysis and generate the results for the mechanisms.

a) Mathematical model of mechanisms under space constrains is obtained under dimensions of different links used in mechanisms
b) CAD modeling of mechanisms in Siemens NX CAD Modeling
c) Discretization of CAD model in Hypermesh
d) Creation of graphic H3D file with defined mass, inertial properties and contacts in Motion View
e) Pre-processing in Motion View
f) Simulating in Motion View
g) Post Processing and generation of the results.

3.7 CAD MODELLING OF DOOR HANDLE MECHANSIM

All the components of the handle mechanism are modeled in Siemen NX 11 PLM software. The slot profile in the rigid support is designed as curve trace by joining the pin point of Link 2 and Link 1 which reduces the size of assembly. The explode view of assembly is given in Fig 3.17.

3.7.1 MASS AND INERTIAL PROPERTIES OF COMPONENTS

Mass, Centre of mass and inertial properties of all components are calculated automatically when CAD/Mesh model is imported in Motion View with respect to a global frame.The material used in door handle is ABS HG173 with density $1.085x10^{-06}$ kg/mm^3, Yield Tensile strength is 46.0913 N/mm^2 and Flexural strength is 74.5305 N/mm^2 with Young's modulus and

flexural modulus of value 235.3596 N/mm^2 and 264.7795 N/mm^2 respectively.

3.7.2 CAD MODEL DISCRETIZATION

CAD Model assembly is first imported to the Hypermesh in parasolid format. A fine 1mm 3D volume R trias mesh is used to discretize the assembly model. In new component, the contact surfaces are extracted from the initial mesh. These surfaces are defined as the contact surface with card image as SURF and followed by the definition of interfaces where two different contact surfaces defined as MASTER and SLAVE with type MBCNTRL. The direction of normal vectors of each contact surface in interference should be against each other. Figure 3.18 shows that the normal vector of two contact surfaces coming out from the surface is towards each other. Extracting the 2D surface mesh from the 3D volume mesh facilitates in defining the contacts between two surfaces in MotionView.

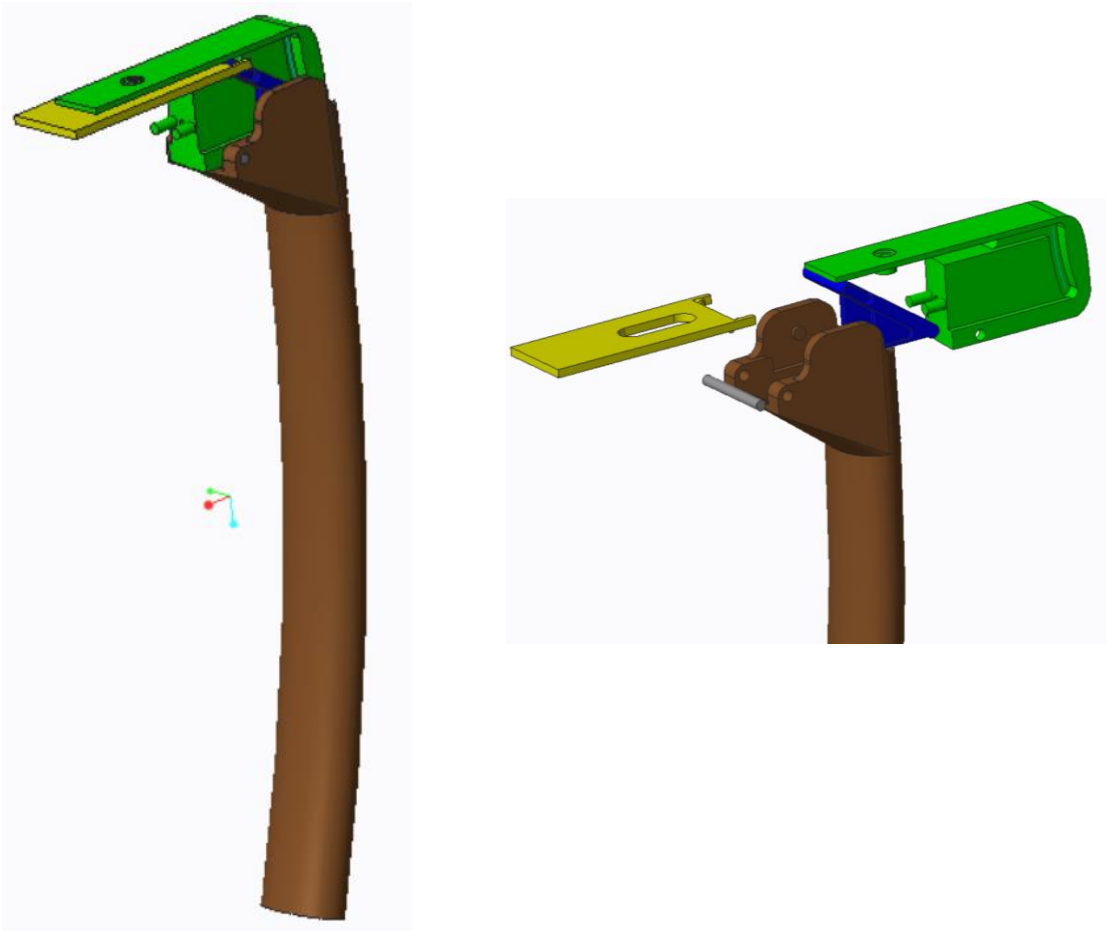

Figure 3.17: CAD Model of Door Handle Assembly

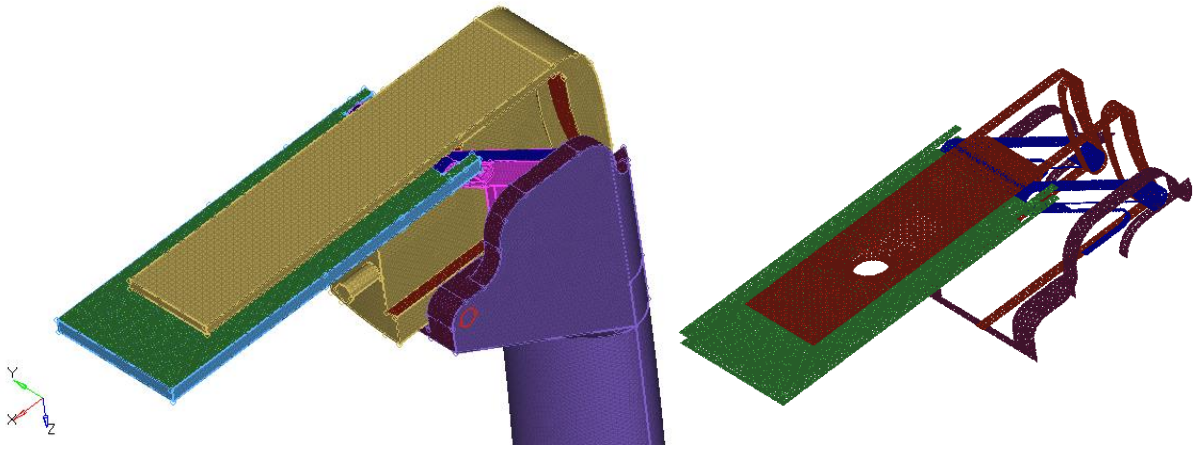

Figure 3.18: Meshed Cad Model and Defined Contact Surfaces

3.7.3 CREATION OF H3D FILE FROM MESH

The file preprocessed in Hypermesh is imported to MotionView tool to convert it into H3D file, which is used to make different parts in H3D. Later, it is used to attach the geometrical graphic. Basic graphic files are created depending on number of collectors used in the meshing. The graphics contact surfaces are defined as a different body in H3D file which are connected to the respective body.

3.7.4 JOINTS

Joints are defined according to motion constraints present in the mechanism. Mainly three types of joints are used in the Multi-body simulation these are two revolute joint, translation joint and fixed joint with respect to the ground. To define the revolute joint it is needed to create point about which the body rotates. Further, select two bodies (lever hand and rigid support, slider and coupler link) in which the rotational motion exist and then select the initially created point to define the axis of rotation. Translation joint is defined between the slider and rigid support. Select centre of gravity as the point of application for translation joint and define the axis of motion as per required conditions. Fixed joints are defined between the rigid support and the ground.

3.7.5 CONTACTS

Contacts are defined between different bodies like coupler link and lever handle, coupler link and slider and coupler link and rigid support slots. The Poisson contacts model is selected to define the contacts between two bodies with properties like restitution coefficient value of 0.05 and penalty value of 3000. The friction between the surface is neglected as the contact travel distance between any two surfaces is too small and it reduces solver time as it reduces the

complexity of model. The value of penalty in Poisson contact model determines the local stiffness between the materials of two bodies, if the value increases, the penetration between two bodies will be more. The coefficient of restitution represents the loss of energy during the collision/contact between the two bodies. For perfectly elastic bodies if the coefficient of restitution value is 1, it represents the zero loss of energy during the contact. Meshed contact surfaces are initially defined in the mesh file however, after importing the mesh file in the MotionView, its required to define the contacts between two bodies with properties. Defined contacts in Motion View are:

1. Poisson Contact model between lever handle and coupler link
2. Poisson Contact model between slider and coupler link
3. Poisson Contact model between Rigid support slot and coupler link

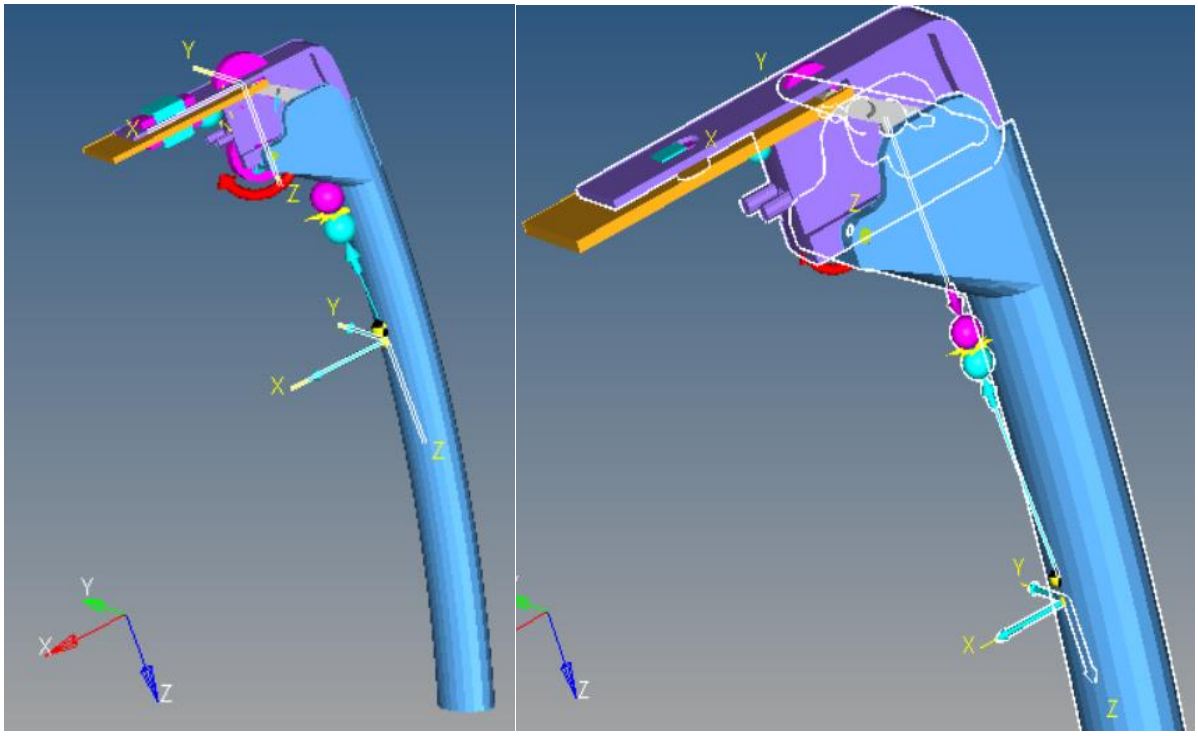

(i) (ii)

Figure 3.19: (i) Defined Markers and Joints and (ii) Poisson Contacts

3.7.6 BOUNDARY CONDITIONS

Here the boundary conditions are referred to motion and force input. A pull force of 10 N is applied on the Centre gravity point of the lever handle and a linear time dependent angular displacement 35^{o}xt where t is time is applied on the revolute joint between the lever handle and the rigid support. Simulation runs are performed for the 1 second in which the movement of the components and force interaction between components are simulated. The results were animated to obtain the forces and displacement of slider.

3.7.7 OUTPUTS

The three required outputs are defined for slider and lever, force require for operating the lever handle, force at transfer to the slider and displacement generated at CG of slider. For this markers are required to be defined. Marker is a coordinate system that is attached to the body or joint on which input and output reading has to be recorded in the simulation. To define a marker, it is required to specify body to which it is attached, origin point the and orientation of the axes for marker. Two markers are defined to record required outputs

1. Marker defined at the revolute joint axis center between slider and link of with respect to ground body. Force and displacement vector are recorded.
2. Marker defined at the point where force is applied on the lever handle with respect to ground body. Only force vector is recorded

3.8 SIMULATION RESULTS

For the designed door opening assist mechanism, the simulation results are obtained. Figure 3.20 shows that the magnitude of force on the revolute joint of slider and coupler link is 68 N near the end of stroke in between 0.600 seconds. The profile obtained from the graph is noisy due to higher value of penalty property Poisson contact model but force profile of slider matches the initial profile obtained from analytical method. As it can be seen in figure 3.21 the peak values of forces on the slide were obtained after 0.800 second simulation when handle is already rotated by 28^{o} angle and it moves towards the zero as it reaches the end.

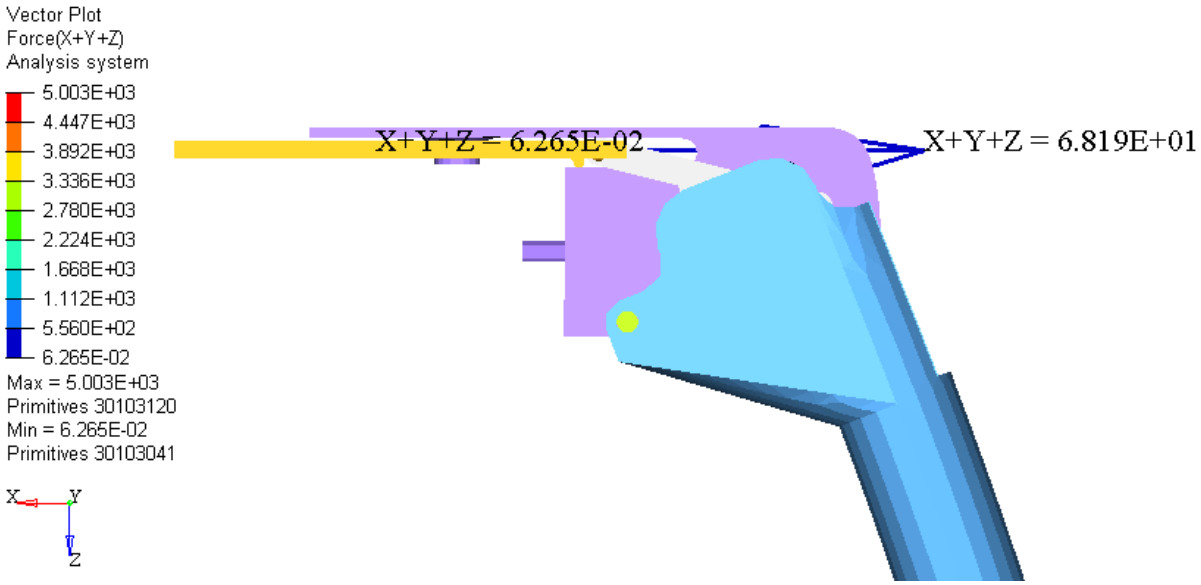

Figure 3.20: Reaction Force Vector at Slider Joints

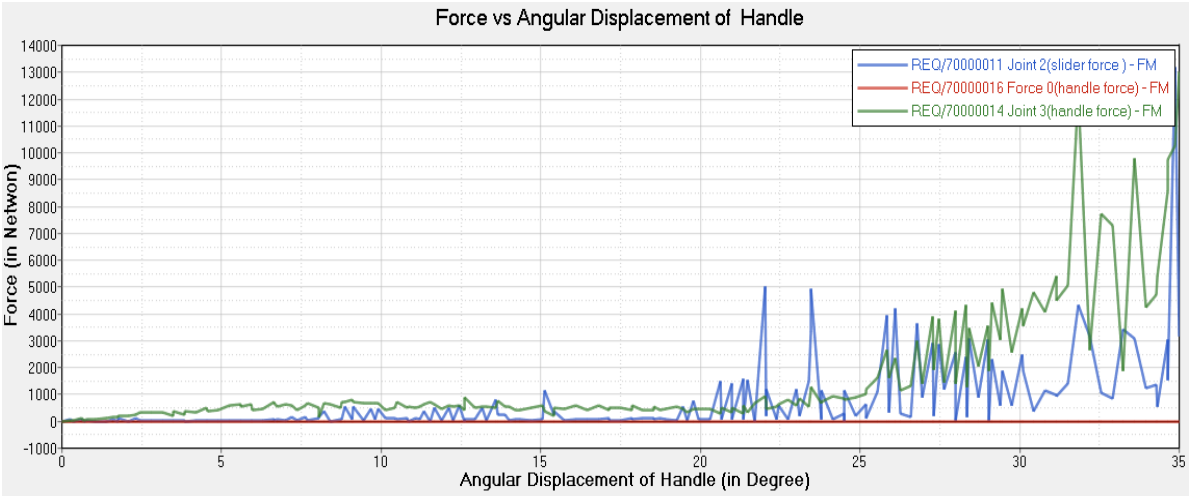

Figure 3.21: Force Profile of Slider and Handle vs. Time

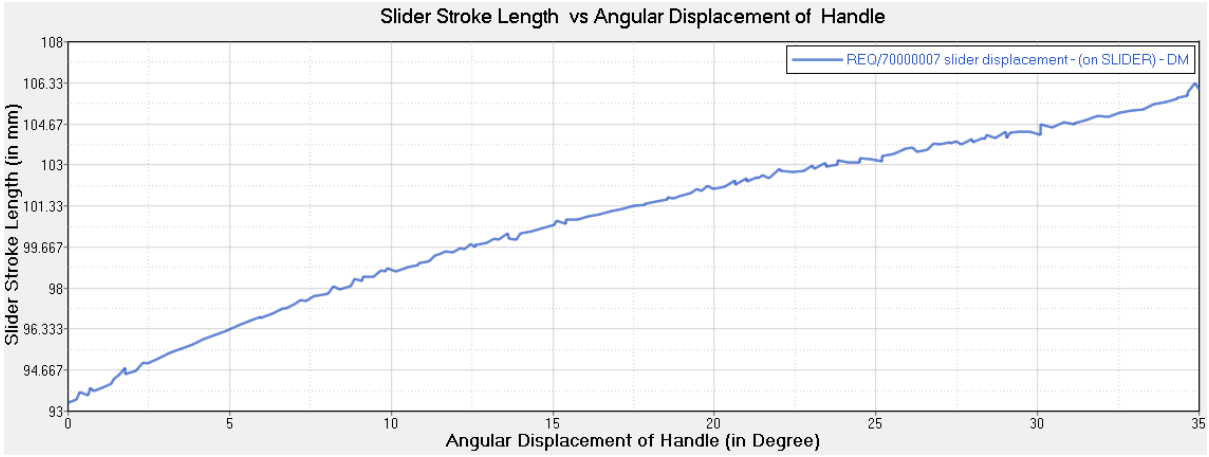

Figure 3.22: Displacement of Slider vs. Time

The Figure 3.22 shows the pattern of displacement curve. It starts with higher rate of change of displacement and in the end the rate of change displacement decrease and amount of output forces at the end of stroke increases rapidly especially in the last 5^{o} degree of the rotating angle of handle lever.

3.9 STRESS ANALYSIS OF DOOR HANDLE PARTS

For the stress analysis of the lever handle and rigid support during initial operating stage of door handle. The face of rigid support jointing the refrigerator door and restricting the movement of the coupler and slider, this is done to create condition when the user is applying the force on the door handle and the output force at the end tip of slider is not enough to oppose the magnetic force of attraction between magnetic gasket and steel door, this restrict the movement of the coupler. Similarly boundary condition applied upon the slider and coupler where their movements where restricted and subjected to 100 N compressive load.

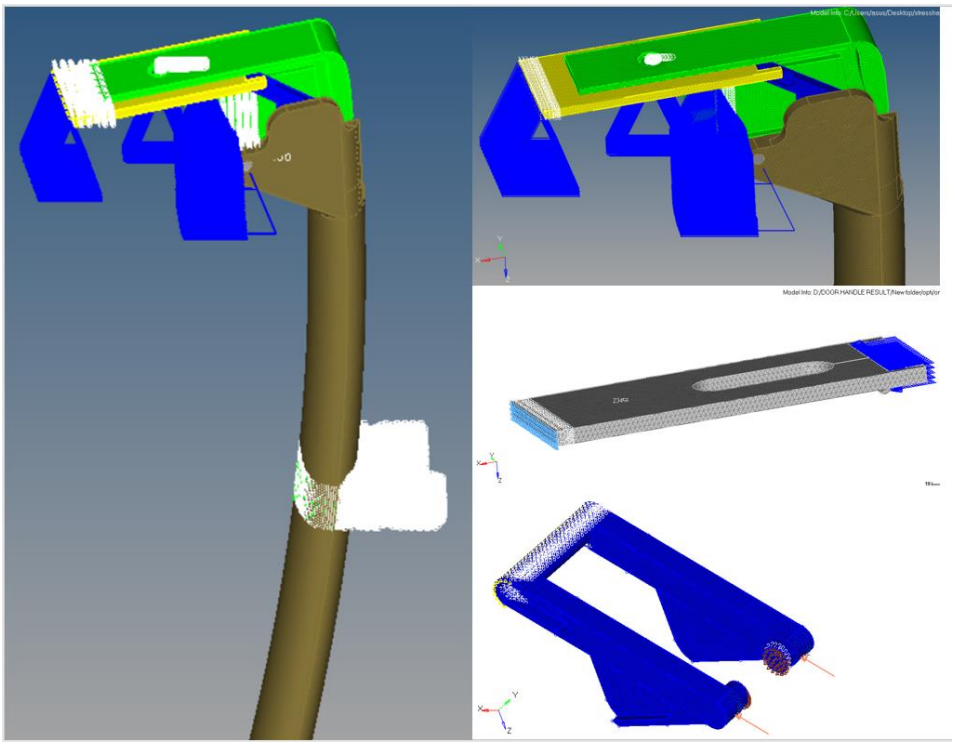

Figure 3.23: Boundary Condition of Door Handle and Components

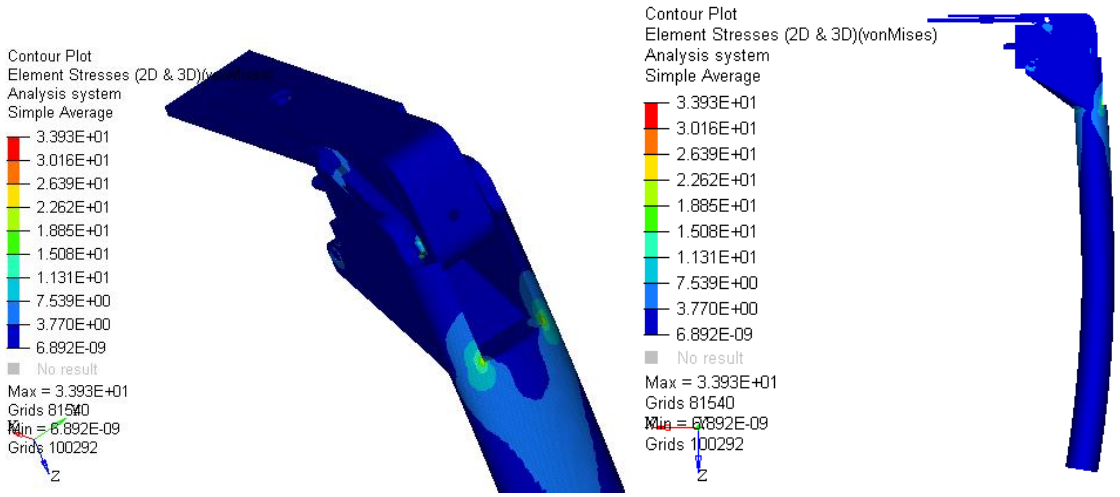

Figure 3.24: Von Mises Stress Analysis of Door Handle Assembly

The door handle is subjected to 50 N pull force and the movement of the slider is restricted is restricted in the assembly as shown in figure 3.23. In the handle assembly, the sliding contact surface are define between two components and a revolute joint is defined in between handle and rigid support. The Maximum Von Mises stresses of 33.93 N/mm^2 occurs at the sharp edges which are very small area, as no fillet is provide to avoid stress concentration in handle. But the maximum stress value is lower than the 47 N/mm^2 yield stress value of ABS HG173.

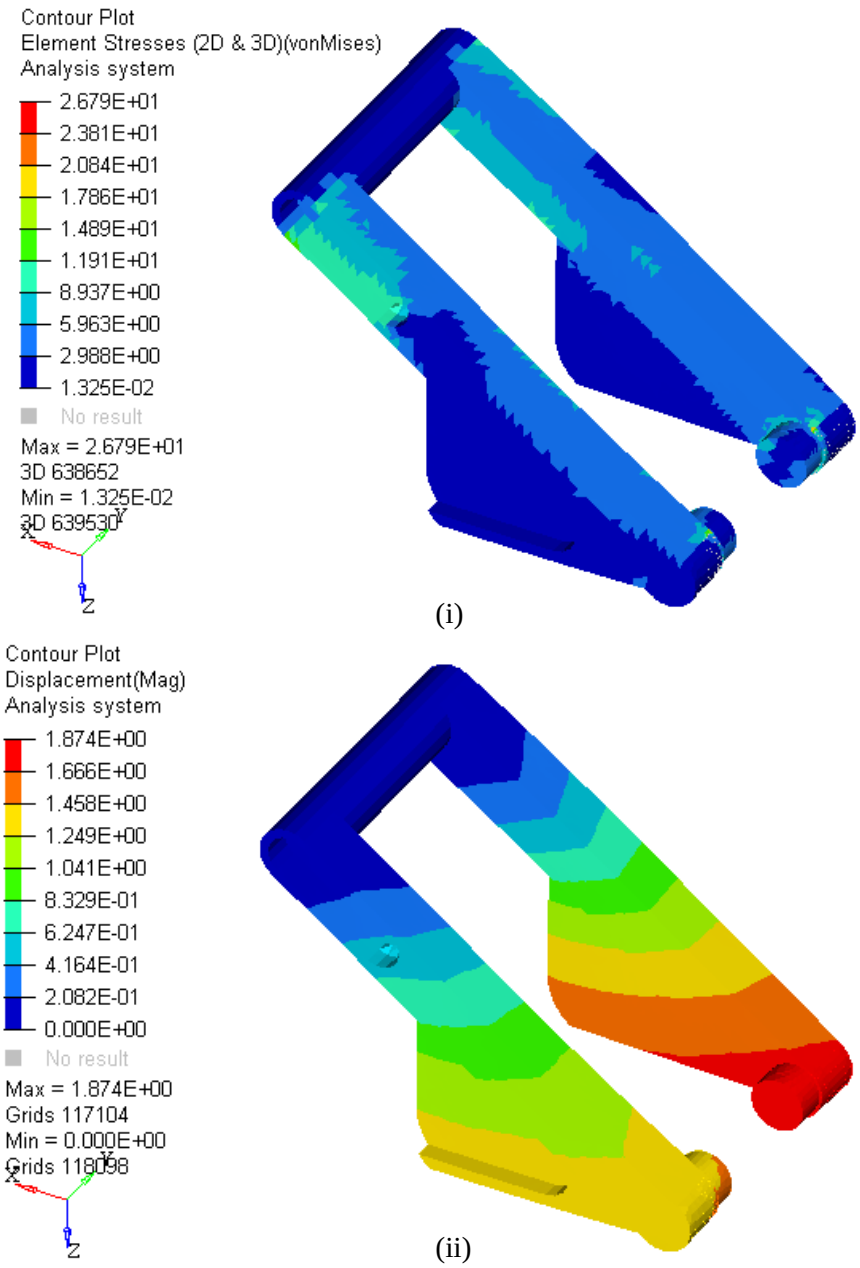

Figure 3.25: (i) Von Mises Stress and (ii) Deformation Analysis of Coupler

Maximum Von Mises Developed in coupler is of magnitude 26.791 N/mm^2 which is approximately half the magnitude of Yield Tensile Strength of ABS HG173. So, it is a safe design and net displacement obtained is of magnitude 1.874 mm. This is very small magnitude and can be neglected

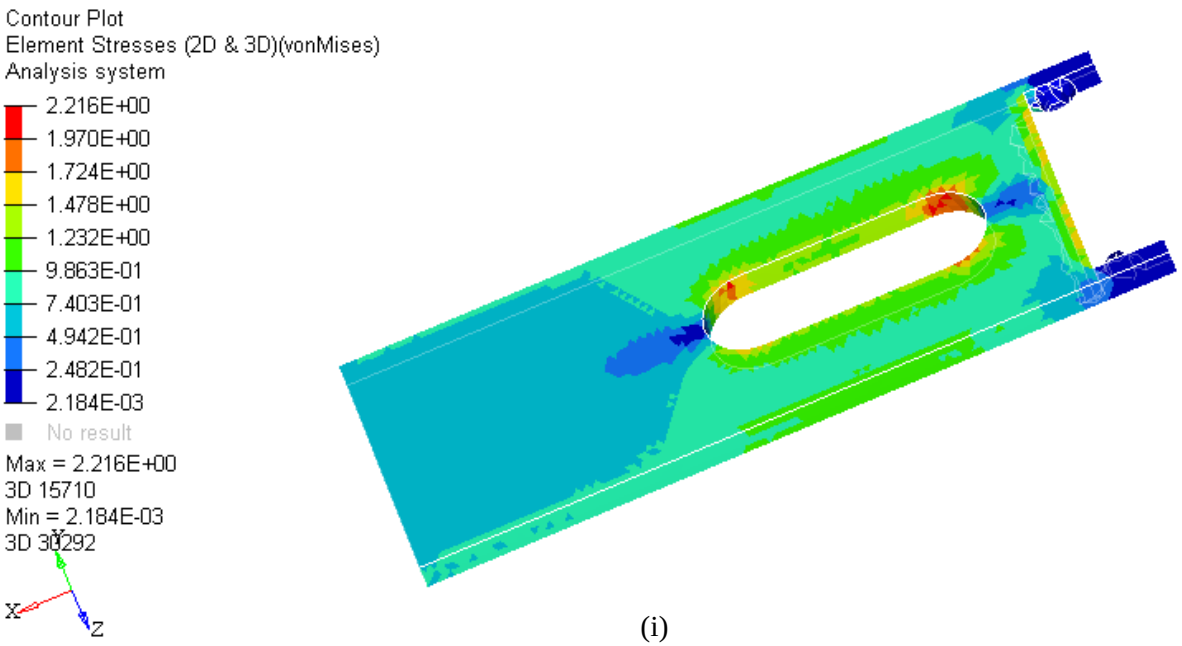

(i)

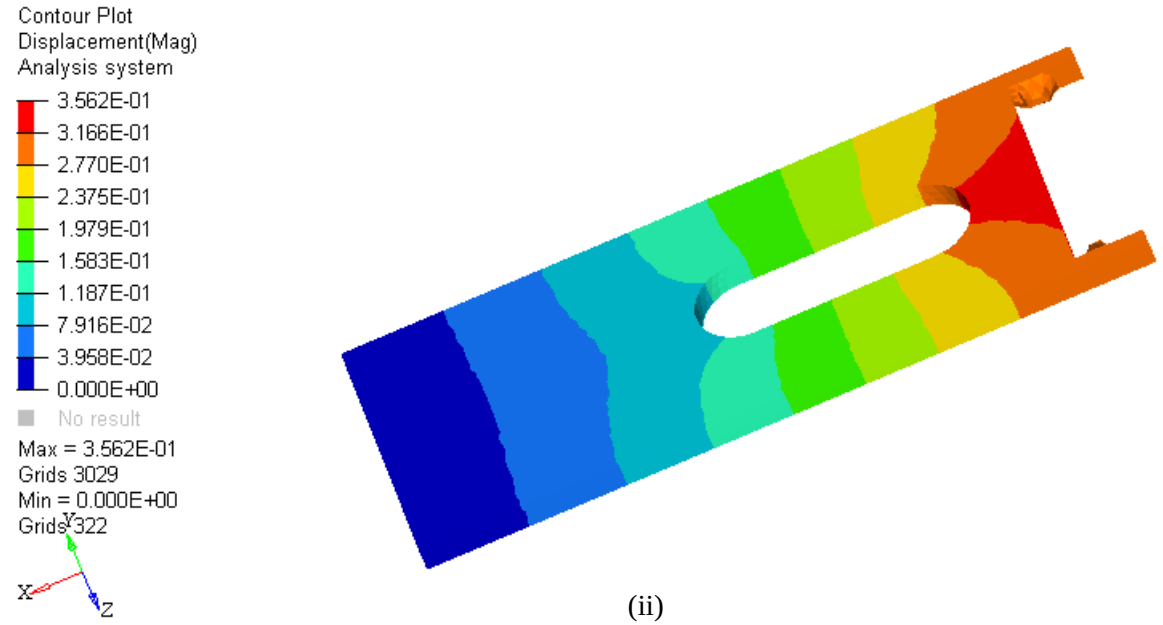

(ii)

Figure 3.26: (i) Von Mises Stress and (ii) Deformation Analysis of Slider

Maximum Von Mises Developed in the slider is of magnitude 2.216 N/mm^2 which is approximately half the magnitude of Yield Tensile Strength of ABS HG173. So, it is a safe design and net displacement obtained is of magnitude 0.3562 mm. This deformation is of very small in magnitude and can be neglected.

3.10 GEARED MOTOR ACTUATOR

Gear motor actuator can be found in many everyday applications like CD driver, CNC Platform and automatic draw opening system etc because of their reliability, efficiency and cost effectiveness. To obtain the required force or torque and motion (linear or rotation), the motor is attached to the gears according to required condition. To obtain the linear motion, the pinion and rack gear combination can be used and the oscillation can also be obtained by using the proper gearbox design as shown in the Figure 3.27. In this design, two half gears were used to obtain the reciprocating motion, rack is directly connected to one half gear for forward motion and for backward motion it is connected to other half gear via a smaller spur gear, as the backward stroke is no force application and it is safer to use smaller gear. As the rack return to its initial position, the power supply to the motor will be terminated and the movement halts at the position where it started. But it is a difficult task to design the gearbox in a given space constrain as it involves many unknown parameters like number of stage in gearbox, gear ration of each stage, pitch diameter of gears and module. There is no defined rule to select the gear ratio for each stage for given gearbox and space constraints. In past literature, the authors purposed the use of genetic algorithm and explicit method to find the gear ratio of each stage within the gearbox based upon the constraints of length, cross section area and volume of the gearbox. This is less time consuming and the results were close to the standard gearbox design procedure. The genetic algorithm is directly applied on the mathematical relations which can be solved by using the computer. Genetic Algorithm provides the global optimized solution for defined domain and constraints.

From the literature, the relationship between the gearbox lengths to the gear ratio of individual stage can be defined by using the gear contact resistance/pitting resistance equation with the function gear's circular pitch diameter (PCD) and torque applied on driving gear. The ratio of the PCD is equal to gear ratio of each stage. The thickness of gearbox is determined by using the maximum allowable bending stress.

Available torque of a small dc motor is 20 Nmm at 6 volt, attached with 10:1 gear ratio worm and worm wheel, to obtain the force of 90 N at end of Rack with stroke length of 100mm. The required net gear ratio is approximately 150. The net gear ratio of 3 stage spur gear set within the box is 15 (the provide gearbox module size constrain is 150 mm x 150 mm). As the input torque is low, the module of all gears in gearbox is kept 1mm constant for all spur gears.

The 150^{o} sector gear of circular pitch diameter of 76 mm and the other 180^{o} sector gear of circular pitch diameter of 64 mm moves the rack gear forward and backward with travelling

stroke of 100 mm. The spur gear in spur gear set four is of pitch circular diameter of 64 mm. All gear are of plastic material Duracon acetal (M90-44) with Young's modulus E=2.7 GPa and allowable contact stress of 49.033 N/mm^2. It is required to keep the sum of $d_{w22}/2$, a_{w2}, a_{w3} and $d_{w44}/2$ to design a compact packing space in which all the component can be arranged.

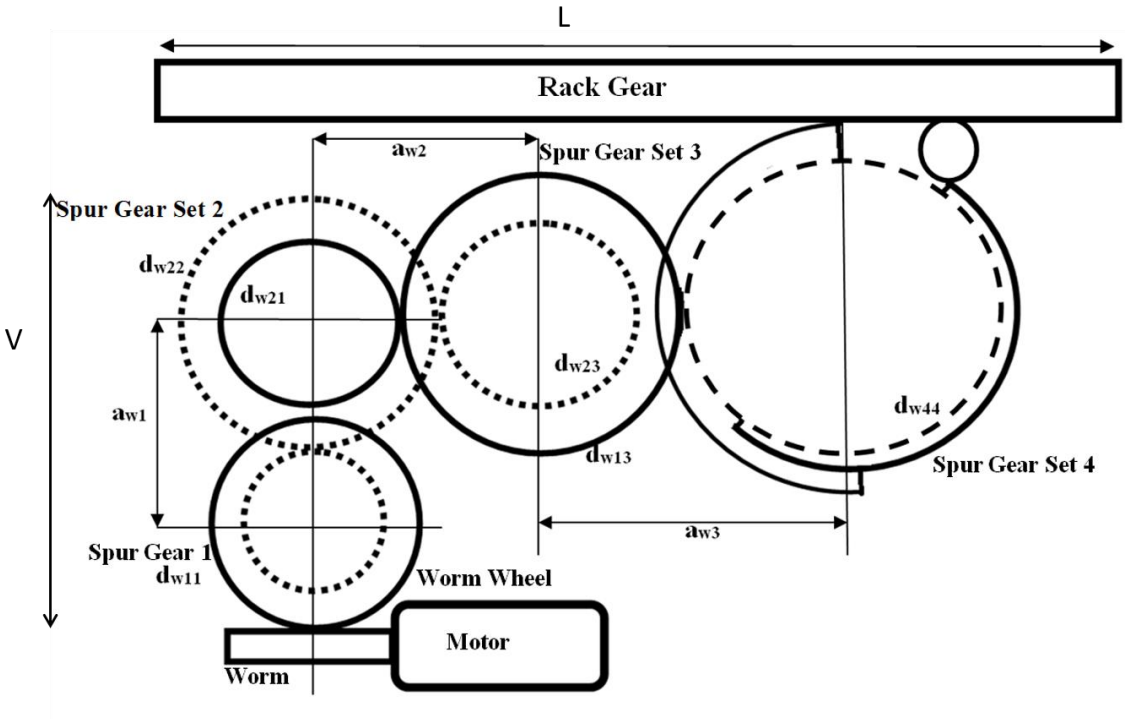

Figure 3.27: Block Diagram of Gear Motor Door Opening Actuator

From the figure 3.27 the net horizontal distance covered by the gears

$$L = \frac{d_{w22}}{2} + a_{w2} + a_{w3} + \frac{d_{w44}}{2} \tag{2.29}$$

Where $a_{w2} = \frac{d_{w12}}{2} + \frac{d_{w13}}{2} = \frac{d_{w13}}{2}\left(\frac{1}{i_2} + 1\right)$ and $a_{w3} = \frac{d_{w23}}{2} + \frac{d_{w44}}{2} = \frac{d_{w44}}{2}\left(\frac{1}{i_3} + 1\right)$ (2.30)

$$L = \frac{d_{w22}}{2} + \frac{d_{w13}}{2}\left(\frac{1}{i_2} + 1\right) + \frac{d_{w44}}{2}\left(\frac{1}{i_3} + 1\right) + \frac{d_{w44}}{2} \tag{2.31}$$

From the figure 3.27 the net vertical distance cover by the gears

$$V = \frac{d_{w22}}{2} + a_{w1} + \frac{d_w}{2} \tag{2.32}$$

Where $a_{w1} = \frac{d_{w11}}{2} + \frac{d_{w22}}{2} = \frac{d_{w22}}{2}\left(\frac{1}{i_1} + 1\right)$

$$V = \frac{d_{w22}}{2} + \frac{d_{w22}}{2}\left(\frac{1}{i_1} + 1\right) + \frac{d_w}{2} \tag{2.33}$$

Using the pitting resistance/contact stress equation for spur gear unit defined in the ISO 6336-2:2006 based upon Hertz equation, following equation is obtained for 1st stage of gear reduction:

$$\sigma_{H1} = Z_{H1}.Z_{E1}.Z_{\beta}.Z_{\varepsilon}.\sqrt{\frac{2.T_{11}.(i_1+1)}{b_{w1}.d_{w11}^2.u_1}} \leq [\sigma_{H1}] \tag{2.29}$$

$$T_{11} = \frac{b_{w1}.d_{w11}^2.u_1.(\sigma_{H1})^2}{2.(i_1+1)\left(Z_{H1}.Z_{E1}.Z_{\beta}.Z_{\varepsilon}\right)^2} \tag{2.35}$$

Where $b_{w1} = \psi_{ba1}.\frac{d_{w22}}{2}\left(\frac{1}{i_1}+1\right)$ and $\frac{d_{w22}}{i_1} = d_{w11}$

$$T_{11} = \frac{\psi_{ba1}.\frac{d_{w11}}{2.i_1}\left(\frac{1}{i_1}+1\right).d_{w11}^2.i_1.(\sigma_{H1})^2}{2.(i_1+1)\left(Z_{H1}.Z_{E1}.Z_{\beta}.Z_{\varepsilon}\right)^2} \tag{2.36}$$

$$T_{11} = \frac{\psi_{ba1}.d_{w22}^3.[K_{01}]}{4\,i_1^2} \tag{2.37}$$

From above equation (2.37) the pitch diameter d_{w22} is

$$d_{w22} = \left[\frac{4.i_1^2.T_{11}}{\psi_{ba1}[K_{01}]}\right]^{\frac{1}{3}} \tag{2.38}$$

Where $K_{01} = \frac{(\sigma_{H1})^2}{\left(Z_{H1}.Z_{E1}.Z_{\beta}.Z_{\varepsilon}\right)^2}$, $Z_{H1} = \sqrt{\frac{2\cos\beta_b\cos\alpha_{wt}}{(\cos\alpha_t)^2\sin\alpha_{wt}}}$, $Z_{E1} = \sqrt{\frac{1}{\pi\left(\frac{1-\vartheta_1^2}{E_1}+\frac{1-\vartheta_2^2}{E_2}\right)}}$,

$$Z_{\varepsilon} = \sqrt{\frac{4-\varepsilon_{\beta}}{3}},\ Z_{\beta} = 1$$

Similarly d_{w13} and d_{w44}

$$d_{w13} = \left[\frac{4.i_2^2.T_{12}}{\psi_{ba2}[K_{02}]}\right]^{\frac{1}{3}} \tag{2.39}$$

$$d_{w44} = \left[\frac{4.i_3^2.T_{13}}{\psi_{ba3}[K_{03}]}\right]^{\frac{1}{3}} \tag{2.40}$$

In the above equations, $Z_{E1}, Z_{H1,} Z_{\varepsilon 1}$ are coefficients which consider the effects of the gear elasticity factor, contact surface shape/zone factor, and contact ratio of the first gear unit when calculate the pitting resistance; $[\sigma_{H1}]$ is allowable contact stresses of spur gear unit; and ψ_{ba1}, ψ_{ba2} and $\psi_{ba3}$are coefficients of spur gear face width which are equal to 0.25 for steps 1,2 and 3 respectively. The T_r is equal to 1/10th of output torque because worm and worm gear ratio is 10.

$$\frac{T_r}{T_{11}} = i_1.i_2.i_3.{n_o}^3, \frac{T_r}{T_{12}} = i_2.i_3.{n_o}^2 \text{ and } \frac{T_r}{T_{13}} = i_3.n_o \tag{2.41}$$

Where n_o is the transmission efficiency of pair of gears in between the range of .99 to .98, let $n_o = .98$.

Substituting the values from eq. (2.35) to eq.(2.31), (2.33) & (2.34) respectively, to obtain

$$d_{w22} = \left[\frac{4.i_1.T_r}{\psi_{ba1}[K_{01}].i_2.i_3.{n_o}^3}\right]^{\frac{1}{3}} \tag{2.42}$$

$$d_{w13} = \left[\frac{4.i_2.T_r}{\psi_{ba2}[K_{02}].i_3.{n_o}^2}\right]^{\frac{1}{3}} \tag{2.43}$$

$$d_{w44} = \left[\frac{4.i_3.T_r}{\psi_{ba3}[K_{03}].i_3.n_o}\right]^{\frac{1}{3}} \tag{2.44}$$

Substituting $d_{w22}, d_{w13}\ and\ d_{w44}$ from into equation (2.31) and (2.32), we get

$$L = \frac{1}{2}\left[\frac{4.i_n.T_r}{\psi_{ba1}[K_{01}].{i_2}^2.{i_3}^2.{n_o}^3}\right]^{\frac{1}{3}} + \frac{1}{2}.\left[\frac{4.i_2.T_r}{\psi_{ba2}[K_{02}].i_3.{n_o}^2}\right]^{\frac{1}{3}}.\left(\frac{1}{i_2}+1\right) + \frac{1}{2}.\left[\frac{4.i_3.T_r}{\psi_{ba3}[K_{03}].n_o}\right]^{\frac{1}{3}}.\left(\frac{1}{i_3}+2\right) \tag{2.45}$$

$$V = \frac{1}{2}.\left[\frac{4.i_1.T_r}{\psi_{ba1}[K_{01}].i_2.i_3.{n_o}^3}\right]^{\frac{1}{3}}.\left(\frac{1}{i_1}+2\right) + \frac{d_w}{2} \tag{2.46}$$

Optimization problem definition

The problem is multi objective problem in which value of L and V needs to be minimized. The objective functions are dependent upon the $i_1,\ i_2$ and i_3.The Genetic Algorithm tool is used to solve the optimization problem within the constrains. The objective functions are defined as equation (2.45) and (2.46). The constraints/fitness functions can be defined as:-

$$1 \leq i_1 \leq \sqrt[3]{i_n} \tag{2.47}$$

$$1 \leq i_2 \leq \sqrt[3]{i_n} \tag{2.48}$$

$$i_3 \geq \sqrt[3]{i_n} \tag{2.49}$$

$$i_n = 15 \tag{2.50}$$

$$i_1 . i_2 . i_3 = 15 \tag{2.51}$$

$$\sigma_H \leq 49.41\ N/mm^2 \tag{2.52}$$

$$dw_{ij} = [16,18,20,24,25,30,32,36,40] \tag{2.53}$$

$$T_r = 3700\ Nmm \tag{2.54}$$

After the optimization of the objective function, the individual stage gear ratio obtained are $i_1 = 1.87, i_2 = 2.37\ and\ i_3 = 3.325$.

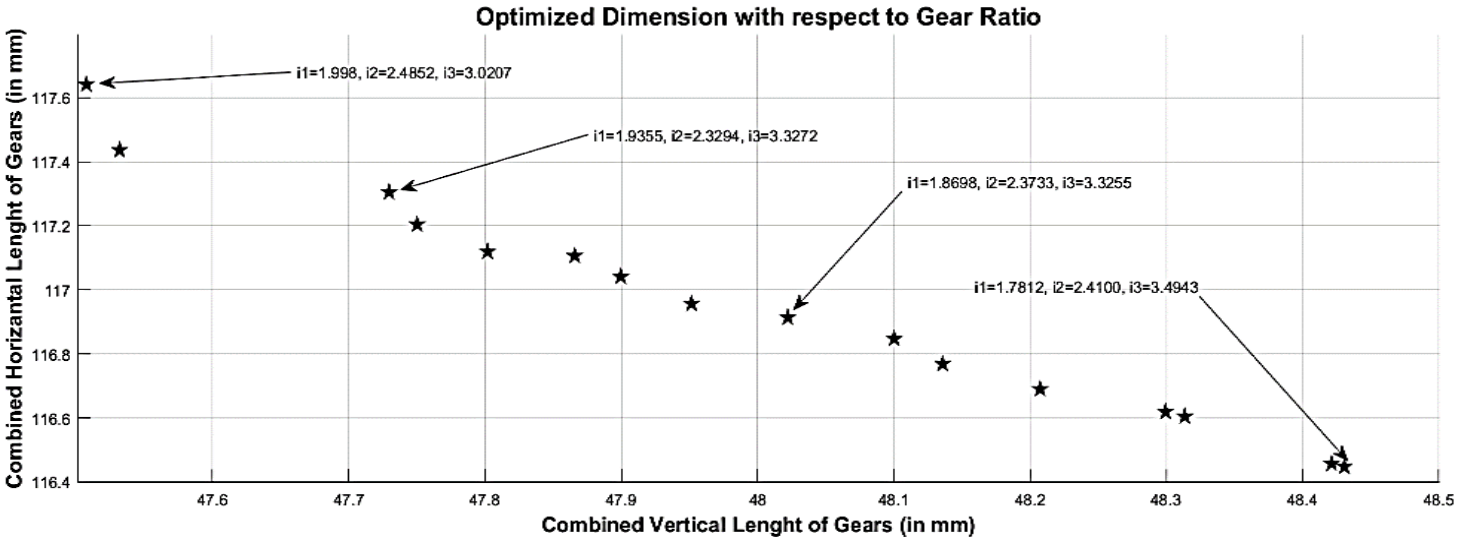

Figure 3.28: MATLAB Genetic Algorithm Result

The pitch diameter of spur gear according to obtained the gear ratios are as: $d_{w11} = 16\ mm, d_{w12} = 30\ mm, d_{w22} = 20\ mm, d_{w13} = 40\ mm\ and\ d_{w23} = 20\ mm$.

As the module for all gears set are kept constant 1mm, so the number of teeth is equal to pitch diameter of spur gear. The above pitch diameter of the spur gears are selected based upon the commercial available spur gear. The net horizontal length of gears in gear box (L) obtained by using above dimension is 117 mm which is less than the 150 mm given length constraint and also less than the length of rack push plunger (140 mm) for compact design and vertical length of gears (V) is 52 mm within constraints space.

CHAPTER 4 EXPERIMENT AND RESULT DISSCUSSION

In this chapter the result of experimental study and simulation result were compared.

4.1 EXPERIMENTAL SETUP

The experimental setup for the design of prototype is build by using 3D printer (Stratasys Fortus 450mc machine) available in the company Proto Lab to check the assembly of designed components with existing refrigerator model and its working. The experimental setup consists of strain gauge, the assembly of newly design door handle and omega 5 refrigerator model. The four point are marked on the handle where the forces will be measured by using strain gauges. The results obtained from the experiment are compared with the simulated/analytically obtained results.

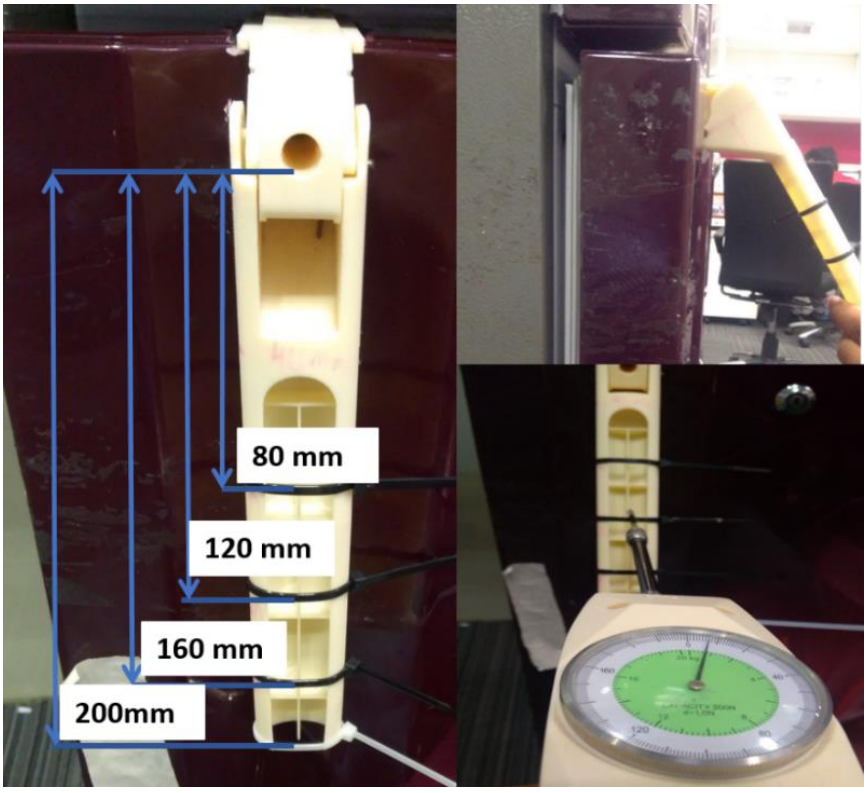

Figure 4.1: Experimental Setup and Reading

4.2 DISCUSSION

The average pull force required to open the door with fixed rigid door handle is approximately equal to 29.7 N but in case of new design it is reduced to 5.3 N at point 120 mm below the hinge of handle. It reduce the force by 5.6 times of original force and no jerk is experienced while operating handle or opening the door of refrigerator. The average mechanical advantage obtained from the analytical method in-between the angular displacement of handle from 0^o to 25^o is 5.97, which is much closed to experimental obtained value 5.6. The design of new door

handle is rigid and strong which can easily with stand the stress induced due to the applied forces.

As the input force decreased, the handle is designed with less amount of material i.e. thickness of walls is less and can be reduced more, some material is already saved as there is no need of extended long handle as compared to initial design which is 500 mm long and present is of 200 mm length. The number of screws also reduced to two from five screws. More material can be reduced by optimizing the thickness of lever handle which will result in the cost reduction.

Table 4.1: Pull Force Reading at Lever Handle at Different Points

Sr. No.	Pull Force Fixed Handle	Pull Force on Moving Handle (80mm below Hinge)		Pull Force on Moving Handle (120mm below Hinge)		Pull Force on Moving Handle (160mm below Hinge)		Pull Force on Moving Handle (200mm below Hinge)	
		Without Spring	With Spring	Without Spring	With Spring	Without Spring	With Spring	Without Spring	With Spring
1	30	8	9	5	6	4	5	3.5	4
2	32	7.5	8.5	5	6.5	4.5	5.5	3	4
3	30	7	9	6	6	4.5	5	3	3.5
4	30	8	9	5.5	6	4	5	3	4
5	28	7	9	5	7	4	5	3	4
6	28	7	8.5	5	6.5	4.5	5	3.5	4
7	30	7.5	8	6	7	4	5	3	4
8	31	7	9	5	6	4	5.5	3	4
9	28	7	9	5.5	6.5	4	6	3	4
10	30	7.5	9	5	6	4	5.5	3.5	3.5

Advantage over First Class Lever Action Mechanism

The amplification of the input force at end of slider remains constant in case of conventional lever action for the overall stroke length. However, for the proposed lever design, the amplification of input force keeps on increasing to infinity as the amplification factor is inverse function of the tangent angle.

The component in the first class lever action used in earlier design and patents is subjected to bending stress under the action of bending moment applied at the handle which increases the probability of failure of components as compared to component under compressive stress. In proposed design, the design components works under the action of compressive load, the probability of failure of part under the compressive stress is lower than tensile stress. Therefore the proposed design has higher life acceptance as compared to the lever action design.

Also, the required raw material cost is reduced by 27% as the handle length is reduced as compare to initial fixed handles length and number of screws are reduced from five to two. However there is need to modify the top deck plate on the door to fit the new design properly.

The new concept design satisfies all the constraints of assembly, packing and position constraint and the prototype of design works properly.

Few modifications are made in the design like slots are provided for guiding purpose to fulfill the assembly constraints and to make the design more rigid by providing extra projection in handle.

Gear motor actuator design fulfills the space constraints and required performance parameter. This design eliminates the need of switch or relay required to change the rotational direction of the motor. The reciprocating motion of rack can be obtained by only one rotational direction of motor. The approach used provides preliminary design of gear drive, further modification can be done to optimize the different module values at different stages and use of helical gear instead of spur gears.

Future Scope of Work

- The proposed new design is designed according to existing assembly and space constraint, but the same configuration of mechanism can be used to make new design.
- There is no material optimization done on the proposed door handle design, so the more material can be removed from it.
- In gear motor door opening design, presently available spur gears were used for basic designing as the cost is considered to be an important factor. To reduce noise during its working, a helical gear can be used instead of spur gears, but it will increase the cost as compared to use of spur gear which can be directly manufactured by plastic injection molding.
- The non circular gear can be used with the triangular plunger rack profile to obtain the gradually increasing push force profile generate at the end of push plunger.

REFERENCES

JOURNALS

Alis A., Majid M.M.A, (2008), "Multibody dynamic analysis and topology optimization of wiper mechanism using Motionview/Motionsolve", *Proceeding of the HTC 2008, India.*

Balli, S.S. and Chand, S., (2002), "Transmission angle in mechanisms (Triangle in mech)", *Mechanism and Machine Theory*, vol 37(2), pp.175-195.

Bauchau O.A., Ju C., (2006), "Modeling friction phenomena in flexible multibody dynamics", *Computer. Methods Applied. Mechanics and. Engineering.* vol. 195, pp. 6909–6924.

Gologlu, C. and Zeyveli, M., (2009). "A genetic approach to automate preliminary design of gear drives". *Computers & Industrial Engineering*, vol *57*(3), pp.1043-1051.

Golabi, S.I., Fesharaki, J.J. and Yazdipoor, M., (2014), "Gear train optimization based on minimum volume/weight design". *Mechanism and Machine Theory*, vol *73*, pp.197-217.

Huang, M.S., Lin, T.Y. and Fung, R.F., (2011), "Key design parameters and optimal design of a five-point double-toggle clamping mechanism". *Applied Mathematical Modelling*, vol *35*(9), pp.4304-4320.

Park, S., Bae, J., Jeon, Y., Chu, K., Bak, J., Seo, T. and Kim, J., (2018), "Optimal design of toggle-linkage mechanism for clamping applications". *Mechanism and Machine Theory*, vol *120*, pp.203-212.

Sutar, A.M. and Shirodkar, V.S., (2015), "Multi-body dynamic analysis of lifting and steering mechanisms", Altair Technology Conference, 2015.

Tanık, E., (2011), "Transmission angle in compliant slider-crank mechanism", *Mechanism and Machine Theory*, vol *46*(11), pp.1623-1632.

Vadhe R., Dave V., (2008), "Multi-body simulation of earthmoving equipment using MotionView / MotionSolve", *Proceeding of the HTC 2008, India.*

Xingguo M., Xiaomei Y., Bangchun W., (2007), "Multi-body Dynamics Simulation on flexible crankshaft system", *Proceeding of the 12th IFToMM World Congress, Besancon, France, June 18th-21th.*

Yoo W.S., Kim M.S., Mun S.H., Sohn J.H., (2006), "Large displacement of beam with base motion: Flexible multibody simulations and experiments*", Computer. Methods Applied. Mechanics and. Engineering*, vol. 195, pp. 7036–7051.

PATENTS

Byeong Gyu Kang, Jeong Ho Shin, Myung Hwan Kim, Sang Bum HA (2013) *United State Patent No. US68444237B2.* Washington, DC: U.S. Patent and Trademark Office.

Gang Hyun Kim, Jin Ho Kim, Seok Jun Son hunji Ueno, Takehisa Okamoto, Yasushi Takagi, Masahiko Maeda, Koichi Nagao (2012) *United State Patent No. US6811236B1.* Washington, DC: U.S. Patent and Trademark Office.

Gang Hyun Kim, Jin Ho Kim, Seok Jun Son (2013) *United State Patent No. US8297725B2.* Washington, DC: U.S. Patent and Trademark Office.

Keith Brookes Spong, Graeme Colin Fuller, Gerald David Duncan (2004) *United State Patent No. US6811236B1.* Washington, DC: U.S. Patent and Trademark Office.

Shunji Ueno, Takehisa Okamoto, Yasushi Takagi, Masahiko Maeda, Koichi Nagao (2013) *United State Patent No. US8297725B2.* Washington, DC: U.S. Patent and Trademark Office.

Yeon-Hark Lee (1999) *United State Patent No.* US5908228A. Washington, DC: U.S. Patent and Trademark Office.

APPENDIX

SolutionPartner

LG Chem

ABS HG173

Injection Molding

Description
High Surface Gloss

Application
Electric&Electronic Products

Properties	Test Condition	Test Method	Unit	Typical Value
Physical				
Specific Gravity		ASTM D792	-	1.05
Molding Shrinkage (Flow), 3.2mm		ASTM D955	%	0.4~0.7
Melt Flow Rate	220℃/10kg	ASTM D1238	g/10min	25
Mechanical				
Tensile Strength, 3.2mm		ASTM D638		
@ Yield	50mm/min		kg/cm^2	470
Tensile Elongation, 3.2mm		ASTM D638		
@ Break	50mm/min		%	40
Tensile Modulus, 3.2mm	1mm/min	ASTM D638	kg/cm^2	24,000
Flexural Strength, 3.2mm	15mm/min	ASTM D790	kg/cm^2	760
Flexural Modulus, 3.2mm	15mm/min	ASTM D790	kg/cm^2	27,000
IZOD Impact Strength, 6.4mm		ASTM D256		
(Notched)	23℃		kg·cm/cm	24
	-30℃		kg·cm/cm	11
IZOD Impact Strength, 3.2mm		ASTM D256		
(Notched)	23℃		kg·cm/cm	25
	-30℃		kg·cm/cm	11
Rockwell Hardness	R-Scale	ASTM D785	-	110
Thermal				
Heat Deflection Temperature, 6.4mm		ASTM D648		
(Unannealed)	18.6kg		℃	85
	4.6kg		℃	89
Vicat Softening Temperature		ASTM D1525		
	5kg, 50℃/h		℃	94
Flammability		UL94		HB
Relative Temperature Index		UL 746B		
Electrical			℃	60
Mechanical with Impact			℃	60
Mechanical without Impact			℃	60

Note) Typical values are only for material selection purpose, and variation within normal tolerances are for various colors.
Values given should not be interpreted as specification and not be used for part or tool design.
All properties, except melt flow rate are measured on injection molulded specimens and after 48 hours storage at 23℃, 50% relative humidty.

Updated : 7-Jun-10

SolutionPartner

LG Chem

ABS HG173

Injection Molding

Description

High Surface Gloss

Application

Electric&Electronic Products

Electrical

Comparative Tracking Index(CTI)	Solution A	IEC 60112	Volts	0
Surface Resistivity		IEC 60093	Ohm	
Volume Resistivity	23℃	ASTM D257	Ohm·m	1.0E+15
Arc Resistance	23℃	ASTM D495	Ohm·cm	6

Note) Typical values are only for material selection purpose, and variation within normal tolerances are for various colors.
Values given should not be interpreted as specification and not be used for part or tool design.
All properties, except melt flow rate are measured on injection molulded specimens and after 48 hours storage at 23℃, 50% relative humidty.

Processing Guide (Injection Molding)

Processing Parameters		Unit	Value
Drying Temperature		℃	80
Drying Time		hrs	2 ~ 4
Minimum Moisture Content		%	0.01
Melt Temperature		℃	210 ~ 240
Cylinder Temperature	Rear	℃	180 ~ 200
	Middle	℃	190 ~ 210
	Front	℃	200 ~ 220
Nozzle Temperature		℃	200 ~ 230
Mold Temperature		℃	40 ~ 70
Back Pressure		kg/cm^2	300 ~ 600
Screw Speed		rpm	30 ~ 60

Note) Back Pressure & Screw Speed are only mentioned as general guidelines.
These may not apply or need adjustment in specific situations such as low shot sizes, thin wall molding and gas-assist molding.

Updated : 7-Jun-10

Document Viewer

Turnitin Originality Report

Processed on: 30-Jul-2018 13:07 +0530
ID: 624141379
Word Count: 13211
Submitted: 45

Navtej By Neeraj Grover

Similarity Index	Similarity by Source	
12%	Internet Sources:	6%
	Publications:	9%
	Student Papers:	3%

include quoted include bibliography excluding matches < 8 words download print

mode: quickview (classic) report

1% match (Internet from 11-Jun-2010)
http://www.cs.nott.ac.uk

1% match (publications)
Saad Mukras, Nam H. Kim, Nathan A. Mauntler, Tony L. Schmitz, W. Gregory Sawyer. "Analysis of planar multibody systems with revolute joint wear", Wear, 2010

1% match (publications)
Huang, M.S.. "Key design parameters and optimal design of a five-point double-toggle clamping mechanism", Applied Mathematical Modelling, 201109

1% match (publications)
Yuan Yunlong. "Optimization design of elbow-bar mechanism in injection molding machine based on genetic algorithm", 2010 2nd International Asia Conference on Informatics in Control Automation and Robotics (CAR 2010), 03/2010

<1% match (student papers from 28-Nov-2017)
Submitted to University of Petroleum and Energy Studies on 2017-11-28

<1% match (publications)
P. Flores. "Introduction", Lecture Notes in Applied and Computational Mechanics, 2008

<1% match (Internet from 15-Jan-2016)
http://www.iaeng.org

<1% match (publications)
Sa'id Golabi, Javad Jafari Fesharaki, Maryam Yazdipoor. "Gear train optimization based on minimum volume/weight design", Mechanism and Machine Theory, 2014

<1% match (publications)
Mathematical Methods in Engineering, 2014.

<1% match (Internet from 16-Jun-2016)
http://documents.mx

<1% match (Internet from 31-Jul-2010)
http://jgap.sourceforge.net